

MOL #67538

THE HIGH-AFFINITY BINDING SITE FOR TRICYCLIC  
ANTIDEPRESSANTS RESIDES IN THE OUTER VESTIBULE OF THE  
SEROTONIN TRANSPORTER

Subhdeep Sarker, René Weissensteiner, Ilka Steiner, Harald H. Sitte,  
Gerhard F. Ecker, Michael Freissmuth\* and Sonja Sucic

SS, IS, HHS, MF and SS are from the Institute of Pharmacology, Center for Physiology  
and Pharmacology, Medical University of Vienna, Waehringer Strasse 13a, A-1090  
Vienna, Austria;

RW and GFE are from the Department of Medicinal Chemistry, University of Vienna,  
Althanstrasse 14, 1090 Vienna, Austria

MOL #67538

(a) Running title: TCA binding sites in monoamine transporters

(b) Corresponding author: Michael Freissmuth, Medical University of Vienna, Institute of Pharmacology, Center for Physiology and Pharmacology, Waehringer Strasse 13a, A-1090 Vienna, Austria; Tel: +43-1-4277-64171; Fax: +43-1-4277-9641

E-mail: [michael.freissmuth@meduniwien.ac.at](mailto:michael.freissmuth@meduniwien.ac.at)

(c) Number of text pages: 35

Number of tables: 0

Number of figures: 7

Number of references: 40

Number of words in the abstract: 251

Number of words in the introduction: 622

Number of words in the discussion: 1088

(d) List of abbreviations:

WIN35,428 or CFT,  $-(-)-2\text{-}\beta\text{-carbomethoxy-3-}\beta\text{-(4-fluorophenyl)tropane}$ ; 5-HT, 5-hydroxytryptamine (serotonin); MDMA,  $s\text{-}(+)\text{-3,4-methylenedioxy-methamphetamine}$ ; MPP<sup>+</sup>, 1-methyl-4-phenylpyridinium ion; PCA, *para*-chloroamphetamine; LeuT<sub>Aa</sub>, leucine transporter from *Aquifex aeolicus*; HEK, human embryonic kidney; DAT, dopamine transporter; NET, noradrenaline transporter; SERT, serotonin transporter; TM, transmembrane segment; YFP, yellow fluorescent protein; CFP, cyan fluorescent protein; GFP, green fluorescent protein.

## ABSTRACT

The structure of the bacterial leucine transporter LeuT<sub>Aa</sub> has been used as a model for mammalian Na<sup>+</sup>/Cl<sup>-</sup>-dependent transporters, in particular the serotonin transporter (SERT). The crystal structure of LeuT<sub>Aa</sub> liganded to tricyclic antidepressants predicts simultaneous binding of inhibitor and substrate. This is incompatible with the mutually competitive inhibition of substrates and inhibitors of SERT. We explored the binding modes of tricyclic antidepressants by homology modeling and docking studies. Two approaches were used subsequently to differentiate between three clusters of potential docking poses: (i) a diagnostic SERT<sup>Y95F</sup> mutation, which greatly reduced the affinity for [<sup>3</sup>H]imipramine but did not affect substrate binding. (ii) Competition binding experiments in the presence and absence of carbamazepine (i.e, a tricyclic imipramine analog with a short side chain that competes with [<sup>3</sup>H]imipramine binding to SERT). Binding of releasers (*para*-chloroamphetamine, methylene-dioxy-methamphetamine/ecstasy) and of carbamazepine were mutually exclusive, but Dixon plots generated in the presence of carbamazepine yielded intersecting lines for serotonin, MPP<sup>+</sup>, paroxetine and ibogaine. These observations are consistent with a model, where: (i) the tricyclic ring is docked into the outer vestibule and the dimethyl-aminopropyl side chain points to the substrate binding site; (ii) binding of amphetamines creates a structural change in the inner and outer vestibule that precludes docking of the tricyclic ring; (iii) simultaneous binding of ibogaine (which binds to the inward-facing conformation) and of carbamazepine is indicative of a second binding site in the inner vestibule, consistent with the pseudo-symmetric fold of monoamine transporters. This may be the second low-affinity binding site for antidepressants.

## INTRODUCTION

The core physiological role of neurotransmitter:sodium symporters (NSS) is to terminate neurotransmission by rapid removal of neurotransmitters from the synaptic cleft and reuptake into presynaptic neurons and/or surrounding glial cells. The subfamily of NSS responsible for the reuptake of monoamines comprises the transporters for noradrenaline (NET), dopamine (DAT) and serotonin (SERT). Structures of these transporters have not yet been solved, but considerable insights have been granted by crystallographic data of their bacterial homolog LeuT<sub>Aa</sub>, isolated from thermophilic bacteria *Aquifex aeolicus*. The first LeuT<sub>Aa</sub> data revealed a high resolution occluded structure devoid of water, with a single leucine (Leu) molecule in coordination with two Na<sup>+</sup> ions (Yamashita et al., 2005). A salt bridge comprising of residues R<sup>30</sup> and D<sup>404</sup> is suggested to act as a barrier between the bound Leu, in the occluded state, and the aqueous pathway connecting the primary binding site to the extracellular bulk solution.

The substrate translocation process was conceptually explained by an alternate access model (Jardetzky, 1966). This model posited a conformational cycle between inward- and outward-facing conformations and thus implicitly predicted a pseudo-symmetry in the transporter molecule. This conjecture was confirmed by the structure of LeuT<sub>Aa</sub> (Yamashita et al., 2005) and other unrelated transporters (Ressl et al., 2009). In LeuT<sub>Aa</sub> the pseudo-symmetrical internal repeats comprise TMs 1-5 and TMs 6-10; TMs 11 and 12 represent a scaffold for this inverted repeat and provide a contact site for the dimeric interface (Yamashita et al., 2005) and this is also true for SERT (Just et al., 2004). Because of its distant relation to monoamine transporters, LeuT<sub>Aa</sub> has been a major

MOL #67538

source of inspiration for educated guesses on the mechanics of the translocation process in monoamine transporters (Shi et al., 2008).

In addition, LeuT<sub>Aa</sub> was also used as template to understand how antidepressants bind to SERT and NET. In fact, the low-affinity interaction sufficed to allow for visualizing tricyclic antidepressants (TCAs), i.e., clomipramine and desipramine, in the extracellular vestibule of the transporter (Singh et al., 2007; Zhou et al., 2007). The LeuT<sub>Aa</sub> co-crystal structures with TCAs reveal a binding pocket harboring Leu and two Na<sup>+</sup> ions (viz., Na<sup>+</sup><sub>1</sub> and Na<sup>+</sup><sub>2</sub>). TCA binding takes place at a site 11Å above the central substrate binding site, thus impeding dissociation of Leu to bulk solution *via* the extracellular pathway. In fact, TCAs are (low-affinity) inhibitors of substrate transport by LeuT<sub>Aa</sub>, but the inhibition is uncompetitive: for instance, clomipramine, at saturating concentrations, slowed [<sup>3</sup>H]leucine dissociation from LeuT<sub>Aa</sub> by up to 700-fold (Singh et al., 2007). This mode of inhibition, however, is incompatible with the competitive inhibition of antidepressant binding to SERT and NET by their substrates and *vice versa*, of substrate translocation by antidepressants.

It has therefore remained a matter of debate whether the observations with LeuT<sub>Aa</sub> are of any relevance to understand how antidepressants bind to the monoamine transporters SERT and NET. Here, we addressed this discrepancy by performing docking of the prototypical TCA imipramine onto a homology model of SERT, based on the LeuT<sub>Aa</sub> structure in the 'open-to-out' conformation (Singh et al., 2008). Docking of imipramine was consistent with the hypothesis that the ring system of TCAs occupied the

MOL #67538

extracellular vestibule of the transporter and the dimethyl-aminopropyl side chain reached deep into the substrate binding pocket. This conjecture was verified by using two approaches: (i) by introducing the Y<sup>95F</sup> mutation to remove the candidate hydrogen bond donating hydroxyl group to the basic side chain nitrogen of imipramine; (ii) by showing that carbamazepine (a tricyclic analogue of imipramine devoid of the long side chain) and serotonin were accommodated simultaneously in SERT. In addition, we identified a second binding site for the tricyclic ring system in the inner vestibule of monoamine transporters, an observation that is consistent with the pseudo-symmetric fold of the transporters.

## MATERIALS AND METHODS

### Alignment and Homology Modeling

The bacterial leucine transporter (LeuT<sub>Aa</sub>) in the 'open-to-out' conformation (PDB accession code 3F3A, Singh et al., 2008) served as the template for building a protein homology model. The sequence alignment between LeuT<sub>Aa</sub> and the primary sequence of hSERT (as given in the UniProt database, entry-code: P31645), based on a comprehensive study on NSS members (Beuming et al. 2006). However, initial models showed K<sup>399</sup> in extracellular loop EL4b pointing into a hydrophobic region. Thus, the alignment was slightly modified, which led to the removal of a gap in the query sequence (**Supplementary Figure 1**). The final models were created using MODELLER 9.4 as implemented in Accelrys Discovery Studio 2.5. Three different modeling runs generating 250 models each have been performed, which included also co-crystallized ligands of the template. These comprise (i) the two Na<sup>+</sup> ions, (ii) the co-crystallized Trp (with removed -COOH group in site1) and, (iii) the co-crystallized tetradecane, located in the extracellular vestibule. The top scored models with respect to DOPE score and PDF score were analyzed with the program PROCHECK (Laskowski et al., 1993). The most favored model showed 93.5% of the residues in allowed regions and 4 residues in disallowed regions. It was additionally assessed on the SWISS-MODEL server (<http://swissmodel.expasy.org/>; Arnold et al., 2006) using the QMEAN scoring function (Benkert et al., 2008). This indicates high accuracy of the homology model in the conserved region of the binding site and parts of the extracellular vestibule (**Supplementary Figure 2**). We also verified that the model was consistent with the results from previous mutagenesis studies, in particular with respect to the location and

## MOL #67538

orientation of residues important for ligand interaction (**Supplementary Table 1**) (Andersen et al., 2009; Barker et al., 1999; Chen and Rudnick, 2000; Field et al., 2010; Forrest et al., 2008; Henry et al., 2003, Henry et al., 2006; White et al. 2006). After manual placement of the two Na<sup>+</sup> ions (at similar position as in the template, Singh et al., 2008) and the Cl<sup>-</sup> ion (based on Forrest et al., 2007; Zomot et al., 2007), partial charges were calculated with MOE 2009.10. Furthermore, hydrogens were assigned with the 'Protonate3d' function of MOE. Subsequently, residues within a radius of 3Å around the ions were minimized (Amber99 forcefield, rms-gradient: 0.1).

### **Docking and evaluation of the poses**

The ligands carbamazepine, di-hydrocarbamazepine, and amitriptyline were built with the molecule builder tool in MOE. Imipramine, clomipramine and desipramine were taken from the crystal structures with the PDB accession codes 2Q72, 2Q6H, and 2QB4, respectively (Singh et al., 2007). Chemical structures for all compounds docked are given in **Supplementary Figure 3**. Initial starting conformations were obtained by protonation of the ligands at pH 7.4 and a stochastic search with the MMFF94x force field. Conformational sampling of the ligands was achieved by short MD-simulations at 2000K for 10ps in MOE. 2000 snapshots were taken every 5fs. After energy minimization the 100 most diverse conformations were taken as input structures for docking. The binding site was defined by using the 'Site Finder' tool in MOE. Residues within a radius of 4.5Å of the generated 'dummy atoms' were selected and were shown to be analogous to those of the template structure (Singh et al., 2008; Zomot et al., 2007). Subsequently, the conformation databases of the selected TCAs were docked into the defined binding site by keeping the protein fixed.



MOL #67538

In order to avoid strong bias caused by scoring functions we fully explored all possible poses by allowing for up to 2300 poses per docking run. Subsequent analysis combined hierarchical clustering, protein ligand interactions and consensus scoring (**Supplementary Figure 4**). First, similar poses were removed by complete linkage clustering based on the RMSD values at a level of 1Å, done with the 'clv' package in R 2.11 (The Comprehensive R Archive Network; <http://cran.r-project.org/>). A first selection criterion based on the 'protein-ligand-interaction-fingerprint' (PLIF), which allows to select poses due to their interaction pattern with the protein. The residues were chosen due to the importance for transporter function (D<sup>98</sup>; Barker et al., 1999), number of poses interacting (E<sup>493</sup>), and location of the residue (Y<sup>95</sup> in the central binding site; Henry et al., 2006, I<sup>179</sup> in the extracellular vestibule; Chen and Rudnick, 2000; Henry et al., 2006). The most frequently populated interacting residues of hSERT with imipramine were E<sup>493</sup>, I<sup>179</sup>, W<sup>182</sup>, R<sup>104</sup>, P<sup>403</sup>, K<sup>490</sup>, Y<sup>95</sup>, and G<sup>442</sup> (decreasing order, see **Supplementary Table 2**). All poses showing contacts with one of the 4 amino acids mentioned above were extracted into separate data bases and minimized with the 'LigX' suite in MOE. This minimisation step allowed slight adaptations of both the ligand and the protein. Subsequently, the minimized complexes were scored by the four scoring functions available in MOE and reclustered at a level of 4Å. The centroid pose and the top scored pose of each cluster was fused into the final database. Finally, the PLIF was calculated for the minimized complexes and used as final filter: only poses with ionic interactions with D<sup>98</sup> or E<sup>493</sup> were considered for final assessment. The resulting 28 poses were visually analyzed. Assuming that simultaneous binding of serotonin and imipramine is

## MOL #67538

not possible, placements without interactions with the central binding site were omitted. 19 poses were finally taken together.

### Materials

Dulbecco's modified Eagle's medium (DMEM) and trypsin were purchased from PAA Laboratories GmbH (Pasching, Austria). Fetal calf serum was purchased from Invitrogen. [<sup>3</sup>H]WIN35,428 ((-)-2-β-[<sup>3</sup>H]carbomethoxy-3-β-(4-fluorophenyl)tropane; 85.9 and 76Ci/mmol), [<sup>3</sup>H]imipramine (47.5Ci/mmol), and [<sup>3</sup>H]5-HT ([<sup>3</sup>H]5-hydroxytryptamine; serotonin; 28.1Ci/mmol) were purchased from PerkinElmer, Boston, MA. [<sup>3</sup>H]MPP<sup>+</sup> (85Ci/mmol) was supplied by American Radiolabeled Chemicals (St Louis, MO, USA). Serotonin (5-HT), s-(+)-3,4-methylenedioxy-methamphetamine (MDMA), paroxetine, carbamazepine and *para*-chloroamphetamine (PCA) were purchased from Sigma. 1-methyl-4-phenylpyridinium ion (MPP<sup>+</sup>) was purchased from Research Biochemicals International, Natick, MA, the polyclonal rabbit antibody directed against GFP was from Abcam PLC, Cambridge. Ibogaine was kindly donated by Sacrament of Transition, Maribor, Slovenia.

### Site-directed mutagenesis, cell culture and transfections

The SERT<sup>Y95F</sup> mutation was generated in the pEYFP-C1-hSERT background (Schmid et al., 2001), using the QuikChange® Lightning site-directed mutagenesis kit (Stratagene, Carlsbad, CA, USA), and confirmed with automatic sequencing (AGOWA Genomics, Berlin, Germany). The primer sequence (5' to 3' sense strands), with the mutated nucleotides indicated in bold font, was: CCTTCTCTCAGTGATTGGC**TTT**GCTGTGGACC. The generation of HEK293 T-REx

## MOL #67538

cells expressing the hSERT under the control of a tetracycline inducible promoter and of the HEK293 cells stably expressing DAT has been described previously (Scholze et al., 2002). For transient expression, HEK293 cells were transfected with wild type or mutant SERT using CaPO<sub>4</sub> co-precipitation. For generation of a stable cell line of SERT<sup>Y95F</sup>, HEK293 cells were transfected using the CaPO<sub>4</sub> co-precipitation method and geneticin (G418, Invitrogen) was added for clone selection.

### **Confocal laser scanning microscopy**

Confocal microscopy was carried out with a Zeiss Axiovert 200-LSM 510 microscope equipped with argon and helium/neon lasers (30 and 1 mW, respectively) and a 40x oil immersion objective (Zeiss Plan-Neofluar). Stably transfected cells (1x10<sup>5</sup> cells/1.6 cm glass coverslip) were placed in a chamber containing Krebs-HEPES buffer. Yellow fluorescent protein (YFP)-tagged proteins were detected with a band pass filter (475-525 nm) using the 458 nm laser line. Images, obtained as z-stacks (slice thickness of ~1µm), were analysed by the LSM Image Browser to study the surface expression of the wild type and mutant SERTs.

### **Radioligand binding assays**

Membranes were prepared from HEK293 cells stably expressing wild type or mutant SERT or DAT as in (Korkhov et al., 2006); expression levels in individual cell clones varied between 4 and 40 pmol/mg; buffers used for the preparation of DAT-expressing membranes contained 10 µM ZnCl<sub>2</sub>-and were devoid of EDTA (because Zn<sup>2+</sup> promotes the outward-facing conformation that is required for high-affinity binding of inhibitors (Scholze et al., 2002). [<sup>3</sup>H]Imipramine equilibrium binding to SERT was performed in

## MOL #67538

duplicate incubations in an assay volume of 0.2 to 0.5 ml (adjusted appropriately to avoid radioligand depletion). In competition binding experiments, membrane preparations (8-25  $\mu\text{g}/\text{assay}$ ) were incubated with the radioligand ( $\sim 2$  nM [ $^3\text{H}$ ]imipramine), the indicated concentrations of carbamazepine and increasing concentrations of a second competing inhibitor in buffer (20 mM Tris-HCl, 1 mM EDTA, 2 mM  $\text{MgCl}_2$ , 3 mM KCl, 120 mM NaCl, pH adjusted to 7.4). Non-specific binding was determined in the presence of 3  $\mu\text{M}$  paroxetine. Saturation experiments were done with serial dilutions of [ $^3\text{H}$ ]imipramine ranging from  $\sim 0.1$  to 50 nM. Equilibrium binding of [ $^3\text{H}$ ]WIN35,428 to DAT was performed in a similar manner but in an assay volume of 0.1 mL containing  $\sim 10$  nM [ $^3\text{H}$ ]WIN35,428 (for competition binding experiments), the indicated concentrations of carbamazepine and ibogaine and buffer (20 mM Tris-HCl, 1 mM  $\text{MgCl}_2$ , 3 mM KCl, 120 mM NaCl, 10  $\mu\text{M}$   $\text{ZnCl}_2$ , pH adjusted to 7.4). In saturation experiments, the concentrations of [ $^3\text{H}$ ]WIN35,428 ranged from  $\sim 1$  to 100 nM. Non-specific binding was determined in parallel in the presence of 3  $\mu\text{M}$  methylphenidate. Binding was allowed to proceed for 15-60 min at 20  $^\circ\text{C}$  and terminated by rapid filtration onto GF/A glass microfiber filters (Whatman<sup>®</sup> International Ltd, Maidstone, UK), presoaked in 0.5% polyethyleneimine (Sigma). The radioactivity trapped on the filter was determined by liquid scintillation counting.

### **Uptake and release assays**

HEK293 cells stably expressing wild type or mutant SERT were seeded onto 48-well plates ( $0.5 \times 10^5$  cells/well), 24 h prior to the experiment. For saturation experiments, the specific activity of [ $^3\text{H}$ ]5-HT was varied between 30 cpm/fmol (0.2  $\mu\text{M}$ ) to 200 cpm/pmol (30  $\mu\text{M}$ ) by addition of unlabeled 5-HT. Assay conditions were as outlined in

## MOL #67538

(Korkhov et al., 2006). For release studies, HEK293 cells stably expressing wild type SERT were grown on coverslips in 96-well plates ( $4 \times 10^4$  cells per well), preloaded with  $0.4 \mu\text{M}$  [ $^3\text{H}$ ]serotonin (specific activity  $\sim 30$  cpm/pmol) or  $0.1 \mu\text{M}$  [ $^3\text{H}$ ]1-methyl-4-phenylpyridinium (MPP $^+$ ,  $\sim 90$  cpm/pmol), for 20 min at  $37^\circ\text{C}$ , in a final volume of 0.1 mL/well. The coverslips were transferred into superfusion chambers and excess radioactivity was washed out with Krebs-HEPES buffer at  $25^\circ\text{C}$ , for 45 min with perfusion rates of 0.7 ml/min. Upon attainment of stable efflux, 2 min fractions were collected for liquid scintillation counting.

### **Immunoblotting**

Membranes were prepared from HEK293 cells stably expressing wild type or mutant SERT or DAT as in (Korkhov et al., 2006). Proteins (10  $\mu\text{g}$ ) were resolved by denaturing gel electrophoresis on a 9% SDS-polyacrylamide gel and subsequently transferred onto a nitrocellulose membrane. The nitrocellulose membrane was blocked with 3% bovine serum albumin (BSA) in Tris-buffered saline (20mM Tris-HCl, pH 7.5, 150mM NaCl) containing 0.1% Tween 20 (TBST), the polyclonal rabbit anti-GFP antibody was used at 1:5000 dilution. Immunoreactive bands were visualized with horseradish peroxidase-coupled anti-rabbit antibody (diluted 1:5000) by enhanced chemiluminescence (reagents from GE healthcare, Little Chalfont, UK).

### **Data analysis**

Data from binding and uptake experiments were subjected to non-linear, least squares curve fitting to equations for a rectangular hyperbola using a Marquardt-Levenberg

MOL #67538

algorithm. The fit was not improved by employing a logistic equation (Hill equation). Data transformed into Dixon plots were fitted by linear regression. Statistical significance was calculated by t-test or Wilcoxon-test as appropriate.

## RESULTS

### Ligand docking shows binding of TCAs in the changeover of site 1 and site 2

Possible binding modes for TCAs were explored by performing docking studies into a homology model of hSERT based on the crystal structure of LeuT<sub>Aa</sub>. The TCA imipramine was docked into the threaded structure using a protocol which exhaustively samples the chemical space for docking poses in the defined binding site. After docking, the most popular interactions were found with residues E<sup>493</sup> (forms with R<sup>104</sup> part of the extracellular gate; Yamashita et al. 2005, Rudnick, 2007), I<sup>179</sup> (one turn above Y<sup>176</sup>, located near the extracellular side of the central binding site; Chen and Rudnick, 2000), W<sup>182</sup> (is located in the extracellular vestibule; White et al., 2006, and conserved in SERT, NET, DAT and LeuT; Beuming et al., 2006), P<sup>403</sup> (is located at the kink in EL4), R<sup>104</sup>, K<sup>490</sup> (one turn above E<sup>493</sup>, towards bulk solution; Andersen et al., 2009), Y<sup>95</sup> (is located at the intracellular side of the central binding site; Henry et al., 2006), and G<sup>442</sup> (in proximity to Y<sup>95</sup>). Out of the 1916 docking poses obtained three distinct clusters of poses were retrieved by analyzing the protein ligand interaction fingerprints (PLIFs), clustering and consensus scoring. Poses of the first cluster show ionic interaction between E<sup>493</sup> and the charged nitrogen of the imipramine side chain as main interaction. These poses are similar to the crystal structures published in 2007 (Singh et al., 2007; Zhou et al., 2007), but the tricyclic ring is buried into the central binding site. Further interactions of the tricyclic ring with the aromatic residues Y<sup>175</sup>, Y<sup>176</sup>, F<sup>335</sup> were observed (**Figure 1a**). In the second cluster the di-benzazepine ring system is placed into the hydrophobic pocket of the central binding site surrounded by I<sup>168</sup>, I<sup>172</sup>, Y<sup>175</sup>, and Y<sup>176</sup> of TM3, V<sup>343</sup> and F<sup>341</sup> of TM6, and T<sup>497</sup> of TM10. The nitrogen atom shows an ionic interaction with D<sup>98</sup>. The ring system shows  $\pi$ - $\pi$  interactions with Y<sup>176</sup> and F<sup>341</sup> (**Figure 1b**). The orientations in cluster

## MOL #67538

3 show the ring system in the extracellular vestibule and the amino propylene side chain rising into the central binding site with an ionic interaction between D<sup>98</sup> and the charged nitrogen. Other interactions are observed between the nitrogen and Y<sup>176</sup> and F<sup>335</sup> (**Figure 1c**). For the sake of clarity it has to be noted that for each cluster only one representative pose is shown. Interacting amino acids were identified with the function “ligand interactions” from MOE and varied slightly for different poses within one cluster (see **Supplementary Table 3** for cluster 3 as example). All these docking poses are consistent with the observation of the competitive inhibition of SERT, but differ in the role of Y<sup>95</sup>: in group 1 docking poses, the dimethyl-aminopropyl side chain points towards the bulk solution (**Figure 1a**); in group 2 and group 3 poses the hydroxyl group of Y<sup>95</sup> is within a distance where hydrogen bonding to the nitrogen in the side chain side of imipramine could be possible, most probably mediated by a structural water molecule as seen in the template. In order to differentiate between these candidate binding modes, we mutated Y<sup>95</sup> to phenylalanine. This choice also appeared justified, because there is a phenylalanine residue in the corresponding position in the NET and DAT. NET and DAT bind imipramine with an affinity that is about 10-fold and 1000-fold lower, respectively, than SERT.

### **The TCA dimethyl-aminopropyl side chain resides in the primary substrate binding pocket**

Previously, it has been shown that Y<sup>95</sup> in the serotonin transporter coordinates high affinity recognition of antidepressants (Henry et al., 2006); accordingly we mutated Y<sup>95</sup> to phenylalanine. We hypothesized the candidate hydrogen bond donor in the hydroxyl group in Y<sup>95</sup> to mediate this high affinity interaction with the TCA side chain. When



MOL #67538

expressed in HEK293 cells, both SERT<sup>WT</sup> and SERT<sup>Y95F</sup> were found predominantly at the cell surface (**Figure 2a**). This indicated the absence of gross misfolding, because incorrectly folded monoamine transporters are retained within the cell (Korkhov et al., 2008). Similarly, the affinity of SERT<sup>WT</sup> and SERT<sup>Y95F</sup> for substrate uptake was comparable (**Figure 2b**;  $K_{M, WT} = 1.2 \pm 0.8 \mu\text{M}$  and  $K_{M, Y95F} = 1.6 \pm 0.8 \mu\text{M}$ ). Differences in  $V_{max}$  of uptake were likely to be accounted for by differences in expression levels (see inset in **Figure 2c**). As expected, removal of the hydroxyl group of Y<sup>95</sup> resulted in a pronounced drop in the affinity of imipramine. This was seen regardless of whether the affinity of imipramine for SERT<sup>Y95F</sup> was determined directly in a binding assay using a membrane preparation (**Figure 2c**, triangles) or *via* inhibition of substrate uptake (**Figure 2d**, triangles). The affinity of SERT<sup>Y95F</sup> for imipramine was lower than that of SERT<sup>WT</sup>;  $K_D$  values were  $6.4 \pm 0.4 \text{ nM}$  and  $46.7 \pm 4.9$  (means  $\pm$  SD,  $n = 4$ ;  $p < 0.01$ ) for SERT<sup>WT</sup> and SERT<sup>Y95F</sup>, respectively. This corresponds to a loss of 1.2 kcal/mol, which is consistent with the contribution of an H-bond to binding free energy (0.5 – 2 kcal/mol). The difference was less pronounced, if imipramine-induced inhibition of serotonin uptake was examined:  $IC_{50}$  values were  $16.3 \pm 1.4 \text{ nM}$  and  $90.9 \pm 20.9 \text{ nM}$  (means  $\pm$  SD,  $n = 4$ ,  $p < 0.01$ ) for SERT<sup>WT</sup> and SERT<sup>Y95F</sup>, respectively.

These observations are consistent with docking poses 2 and 3 but are incompatible with docking pose group 1. Specifically, the results argue for a role of hydrogen bonding between the hydroxyl group of Y<sup>95</sup> to the nitrogen in the dimethylaminopropyl side chain of imipramine. In the case of cluster 2 poses, the dimethylammonium group more likely interacts via cationa/ $\pi$ -interaction rather than *via* an H-bond. This would also rule out

## MOL #67538

docking poses 2. However, one has to bear in mind that both the dimethylaminopropyl side chain as well as the tyrosine are highly flexible moieties and thus could accommodate orientations which also allow for H-bonding. Thus, to further validate our experimental results we sought for a complementary approach: the tricyclic compounds carbamazepine and di-hydrocarbamazepine were docked into the structural model of SERT: di-hydrocarbamazepine has the same ring system as imipramine but the dimethylaminopropyl side chain is replaced by a carboxamido group. In carbamazepine, the flexibility of the central epine ring is restricted by a double bond. In the main groups of docking poses carbamazepine and di-hydrocarbamazepine were found to occupy similar positions as that of the tricyclic ring system of imipramine, desipramine and amitryptiline (**Figure 3**).

### **Carbamazepine and imipramine share a common binding pocket in SERT**

The docking studies predicted that carbamazepine ought to compete with imipramine for binding to SERT. This prediction was verified by two approaches. (i) Saturation experiments with [<sup>3</sup>H]imipramine were carried out in the presence of increasing concentrations of imipramine (**Figure 4a**). Carbamazepine caused a rightward shift in the saturation curve of [<sup>3</sup>H]imipramine in a manner that was consistent with competitive inhibition. This is most readily evident from the Schild-plot depicted in **Figure 4b**: the slope of the Schild regression (1.13) was close to unity and the intercept with the x-axis gave a pK<sub>B</sub> of 2.03, i.e. an affinity estimate of 93 μM for carbamazepine. (ii) Alternatively, carbamazepine was allowed to compete for [<sup>3</sup>H]imipramine binding at two different concentrations of the radioligand (i.e., 0.8 and 9.9 nM). The shift in the apparent IC<sub>50</sub>-values (119±15 μM vs. 563±61 μM) at 0.8 and 9.9 nM [<sup>3</sup>H]imipramine,

## MOL #67538

respectively;  $n=3$ ) was consistent with that predicted from the Cheng-Prusoff equation ( $K_i = IC_{50}/[1+L/K_D]$ ). The resulting affinity estimates  $K_i$  were in the range of 85 to 95  $\mu\text{M}$  and thus consistent with the affinity estimate obtained from the Schild regression. We also investigated di-hydrocarbamazepine: it also inhibited [ $^3\text{H}$ ]imipramine binding albeit with a lower affinity than carbamazepine (not shown).

Carbamazepine was reported to cause serotonin release from brain slices in a manner independent of an action on SERT (Dailey et al., 1997). We confirmed that carbamazepine *per se* failed to release [ $^3\text{H}$ ]serotonin from SERT-expressing preloaded HEK293 cells (**Figure 4d**). However carbamazepine blunted serotonin-release induced by *para*-chloroamphetamine (**Figure 4d**). This observation is consistent with the ability of carbamazepine to occupy the imipramine binding site of SERT and to thereby antagonize the releasing action of amphetamines.

### **Substrates and inhibitors bind to SERT in a mutually non-exclusive manner in the presence of carbamazepine**

Docking pose groups 2 and 3 can thus be differentiated by the position of carbamazepine relative to the substrate binding site: in group 3, carbamazepine allows for simultaneous occupancy of the substrate binding site, because it lacks the aliphatic dimethylaminopropyl side chain of imipramine. In contrast, in group 2 docking poses, carbamazepine would occupy the substrate binding site properly. Serotonin was allowed to compete for [ $^3\text{H}$ ]imipramine in the absence and presence of carbamazepine to differentiate between these two binding modes (**Figure 5a**). Dixon plots (where the reciprocal of bound radioactivity is plotted as a function of one inhibitor at a fixed

MOL #67538

concentration of the second inhibitor) allow to test if two inhibitors can occupy the same binding site simultaneously or whether their binding is mutually exclusive (Segel, 1975). When the data summarized in **Figure 5a** were replotted in a Dixon plot, they fell onto lines that pivoted around an intersection point close to the x-axis (**Figure 5b**). This was also seen in membranes prepared from cells that expressed SERT at 10-fold higher density (**inset to Figure 5b**). If two inhibitors compete for the same binding site, their binding is mutually exclusive and this results in parallel lines in the Dixon plot. Conversely, if both inhibitors can be bound simultaneously, Dixon plots are expected to yield intersecting lines (Segel, 1975). Thus the data unequivocally show that binding of serotonin and carbamazepine is not mutually exclusive. Similar observations were also made with 1-methyl-4-phenylpyridinium ion (MPP<sup>+</sup>), another substrate of SERT (data not shown). SERT is also inhibited by a class of compounds that are collectively referred to as selective serotonin reuptake inhibitors (SSRI's). These are structurally unrelated to TCAs. Several recent modeling studies argued for binding of SSRI's to the substrate binding site (Andersen et al., 2010; Tavoulari et al., 2009). If these assignments were correct, all our experiments would be consistent with a model, where simultaneous binding of carbamazepine and paroxetine ought to be possible. This conjecture was tested by measuring paroxetine-induced inhibition of [<sup>3</sup>H]imipramine binding in the absence and presence of carbamazepine. A Dixon plot of the inhibition curves again yielded a family of intersecting lines (**Figure 6a**) showing that carbamazepine and paroxetine occupy mutually non-exclusive binding sites in the transporter.

### **Mutually exclusive binding of *para*-chloroamphetamine and MDMA to SERT but not of ibogaine in the presence of carbamazepine**

Amphetamines are inwardly transported substrates of monoamine transporters that trigger serotonin efflux. While the details remain enigmatic (Sitte and Freissmuth, 2010), it is clear that the conformation of SERT in its amphetamine bound state must differ from that of the serotonin-or MPP<sup>+</sup>-liganded conformation. We therefore explored if carbamazepine and methylene-dioxy-*N*-methylamphetamine (MDMA, "ecstasy") or *para*-chloroamphetamine were bound simultaneously: in the presence of carbamazepine, we observed a parallel shift in the Dixon plots for both, MDMA (**Figure 6b**) and *para*-chloroamphetamine (**Figure 6c**). This is diagnostic of mutually exclusive binding of carbamazepine and amphetamines.

We also examined ibogaine another ligand of SERT, which has previously been shown to stabilize SERT in the inward-facing conformation (Jacobs et al., 2007). Because binding of imipramine and carbamazepine is to the outward-facing conformation, ibogaine and carbamazepine are not predicted to be bound simultaneously. Surprisingly, this was not the case (**Figure 7**). In the presence of ibogaine, we observed that the inhibition curves generated in the absence and presence of carbamazepine intersected when replotted as Dixon plots (**Figures 7b, d**). This was seen regardless of whether we examined the interaction of the two compounds in SERT (**Figures 7a, b**) or in DAT (**Figures 7c, d**). This finding can be rationalized by considering the pseudo two-fold axis symmetry predicted to exist for NSS transport proteins (Ressler et al., 2009; Singh et al., 2008; Yamashita et al., 2005). A second binding site may exist in the inner vestibule that can

MOL #67538

accommodate the tricyclic ring of carbamazepine if ibogaine is bound to the substrate binding site in the inward-facing conformation. It is worth noting that a second (low affinity) binding site has previously been described for imipramine in SERT (Schloss and Betz, 1995).

## DISCUSSION

Tricyclic antidepressant drugs were instrumental in the discovery of neurotransmitter reuptake and – in conjunction with other drugs and chemicals - in the dissection of the underlying mechanisms (Hertting and Axelrod, 1961). The serotonin transporter has remained a prime target for antidepressant drugs since this seminal discovery. It has remained enigmatic how these drugs bind, because the transporter can accommodate a bewildering variety of structures. Based on the recent work with the bacterial homologue LeuT<sub>Aa</sub>, two binding sites have been proposed (**Supplementary Figure 5**): (i) a vestibular binding site (Singh et al., 2007; Zhou et al., 2007) that also functions as a secondary substrate binding site (Shi et al., 2008). (ii) the substrate binding site *per se* (Andersen et al., 2010; Tavoulari et al., 2009); the latter assignment is also supported by a combination of computer-assisted modeling and site directed mutagenesis studies which suggest that cocaine analogs occupy the substrate binding pocket in DAT (Beuming et al., 2008).

The importance of the vestibular binding site has been a matter of debate. It can, for instance, be argued that the low affinity of tricyclic antidepressants (TCAs) for LeuT<sub>Aa</sub> render these models questionable. In fact at the concentrations range in which tricyclic antidepressants bind to LeuT<sub>Aa</sub> they also bind to many other targets including mammalian Na<sup>+</sup>- and K<sup>+</sup>-channels and numerous G protein-coupled receptors. At the current stage, it would seem doubtful that any insight can be gained from the vestibular binding of desipramine to LeuT<sub>Aa</sub> that would be relevant to understand the function of the pore region of the Na<sup>+</sup>-channel. Here, we have used an approach that combines docking

MOL #67538

studies and site-directed mutagenesis with a chemical biology approach, namely the use of the tricyclic compound carbamazepine to prioritize docking hypotheses. Carbamazepine can be viewed as a truncated version of imipramine rendered more rigid by the presence of a double bond in the central epine ring. The underlying rationale is the assumption that carbamazepine and imipramine compete for the same binding site, i.e. the site to which the tricyclic ring system docks. Our experiments provided formal proof for this assumption: in two independent assays, carbamazepine fulfilled the criteria of a (low affinity) competitive inhibitor of [<sup>3</sup>H]imipramine binding. In addition, it blunted amphetamine induced reverse transport. It is worth noting that there are several ways by which carbamazepine and TCAs can be docked into the SERT model: however, assuming a common binding mode for the dibenzazepine ring system, there is only one group of docking poses that allows for simultaneous binding of carbamazepine and substrate: one in which the tricyclic ring is placed in the outer vestibule and the basic side chain points into the direction of the substrate binding site (docking pose group 3; Figure 1c and Figure 3). This explains both the mutually exclusive binding of imipramine and serotonin and the non-exclusive binding of carbamazepine and serotonin. It is worth noting that the top scored docking poses, which belong to group 1 (**Figure 1a**), would be consistent with the orientation of desipramine and clomipramine in the vestibule of LeuT<sub>Aa</sub> (Singh et al., 2007; Zhou et al., 2007). However, it is nevertheless highly likely that this is not the correct orientation: the drop in [<sup>3</sup>H]imipramine affinity that resulted Y<sup>95F</sup> mutation cannot be accounted for by this orientation but is readily explained by the loss of a hydrogen bond between the hydroxyl group of the tyrosine side chain at residue Y<sup>95</sup> and the tertiary amine in the dimethyl-aminopropyl group of imipramine. The importance of Y<sup>95</sup> of SERT



## MOL #67538

for the binding of tricyclic drugs was originally appreciated based on a substitution by cysteine (Henry et al., 2006), removing the phenyl ring and introducing a side chain can alter the flexibility of the helices by hydrogen bonding to main chain amide bonds one helical turn removed. The replacement of tyrosine with phenylalanine however, is more subtle and sufficed to greatly reduce the affinity of imipramine (but not of serotonin). We are aware that, in our model, the distance between the hydroxyl of the tyrosine residue and the tertiary amine of imipramine is *a priori* too large for forming a hydrogen bond. However, the LeuT<sub>Aa</sub> template structure used for homology modeling shows a structural water molecule interacting with N<sup>21</sup>, which is analogous to Y<sup>95</sup> in SERT. This structural water molecule could thus mediate the hydrogen bond between Y<sup>95</sup> and imipramine. Thus, taken together our observations are consistent with the presence of two overlapping binding sites in SERT: the tricyclic ring system is in the outer vestibule and the dimethylaminopropyl side chain reaches into the substrate binding site. Other inhibitors (i.e., SSRI's) must bind in distinct modes in this region to account for the observation that binding of paroxetine and carbamazepine was not mutually exclusive. The presence of two binding communicating sites can also be inferred from the increase in affinity and blocking efficacy seen with bivalent phenethylamines (Schmitt et al., 2010).

Our approach also allowed for probing the effect of amphetamines on the conformation of the binding pocket. Amphetamines are also subject to inward transport by SERT (and the other monoamine transporters), but they alter the conformation of the transporter in a way that allows for substrate efflux (Sitte and Freissmuth, 2010). Earlier experiments suggested counter-transport mechanism contingent on the oligomeric arrangement of

MOL #67538

transporters (Seidel et al., 2005) and an important role of serine/threonine-kinase-mediated phosphorylation of residues in the N-terminus of DAT and SERT (Fog et al., 2006). Recent experiments indicate that the N-terminus may possibly function as a lever (Sucic et al., 2010) in a manner analogous to that seen in BetP (Ressl et al., 2009) and to thereby afford the communication between the individual moieties within the transporter oligomers. The issue is to understand how the N-terminus senses that an amphetamine – rather than serotonin – resides within the substrate binding site and the permeation pathway. Our observations show that carbamazepine cannot be accommodated by SERT in the amphetamine-bound state. The conformation of the amphetamine-bound state can also be inferred to be distinct from the inward-facing conformation: the latter is stabilized by ibogaine (Jacobs et al., 2007). The ibogaine-bound conformation, however, allowed for simultaneous binding of carbamazepine to a site that may correspond to the second, low-affinity imipramine binding site (Schloss and Betz, 1995). Thus, in the presence of amphetamine, neither the inner nor the outer vestibule is accessible to carbamazepine. This conformation is therefore fundamentally different from the serotonin-bound state. It will be interesting to explore how the change in the inner vestibule is transmitted to the N-terminus of SERT (and of other monoamine transporters).

## REFERENCES

- Andersen J, Olsen L, Hansen KB, Taboureau O, Jørgensen FS, Jørgensen AM, Bang-Andersen B, Egebjerg J, Strømgaard K, and Kristensen AS (2010) Mutational mapping and modeling of the binding site for (S)-citalopram in the human serotonin transporter. *J Biol Chem* **285**:2051-2063.
- Andersen J, Taboureau O, Hansen KB, Olsen L, Egebjerg J, Strømgaard K, and Kristensen AS (2009) Location of the antidepressant binding site in the serotonin transporter: importance of Ser-438 in recognition of citalopram and tricyclic antidepressants. *J Biol Chem* **284**:10276-10284.
- Arnold K, Bordoli L, Kopp J, and Schwede T (2006) The SWISS-MODEL Workspace: A web-based environment for protein structure homology modelling. *Bioinformatics* **22**:195-201.
- Barker EL, Moore KR, Rakhshan F, and Blakely RD (1999) Transmembrane domain I contributes to the permeation pathway for serotonin and ions in the serotonin transporter. *J Neurosci* **19**:4705-4717.
- Beuming T, Kniazeff J, Bergmann ML, Shi L, Gracia L, Raniszewska K, Newman AH, Javitch JA, Weinstein H, Gether U, and Loland CJ (2008) The binding sites for cocaine and dopamine in the dopamine transporter overlap. *Nat Neurosci* **11**:780-789.
- Beuming T, Shi L, Javitch JA, and Weinstein H (2006) A comprehensive structure-based alignment of prokaryotic and eukaryotic neurotransmitter/Na<sup>+</sup> symporters (NSS) aids in the use of the LeuT structure to probe NSS structure and function. *Mol Pharmacol* **70**:1630-1642.
- Benkert P, Tosatto SC, and Schomburg D (2008) QMEAN: A comprehensive scoring function for model quality assessment. *Proteins* **71**:261-277.
- Chen JG, and Rudnick G (2000) Permeation and gating residues in serotonin transporter *Proc Natl Acad Sci U S A*. **97**:1044-1049.
- Dailey JW, Reith ME, Yan QS, Li MY, and Jobe PC (1997) Carbamazepine increases extracellular serotonin concentration: lack of antagonism by tetrodotoxin or zero Ca<sup>2+</sup>. *Eur J Pharmacol* **328**:153-162.
- Field JR, Henry LK, and Blakely RD (2010) Transmembrane domain 6 of the human serotonin transporter contributes to an aqueously accessible binding pocket for serotonin and the psychostimulant 3,4-methylene dioxymethamphetamine. *J Biol Chem* **285**:11270-11280.
- Fog JU, Khoshbouei H, Holy M, Owens WA, Vaegter CB, Sen N, Nikandrova Y, Bowton E, McMahon DG, Colbran RJ, Daws LC, Sitte HH, Javitch JA, Galli A, and Gether U (2006) Calmodulin kinase II interacts with the dopamine transporter C terminus to regulate amphetamine-induced reverse transport. *Neuron* **51**:417-429.
- Forrest LR, Zhang YW, Jacobs MT, Gesmonde J, Xie L, Honig BH, and Rudnick G (2008) Mechanism for alternating access in neurotransmitter transporters. *Proc Natl Acad Sci U S A* **105**:10338-10343.
- Forrest LR, Tavoulari S, Zhang YW, Rudnick G, and Honig B (2007) Identification of a chloride ion binding site in Na<sup>+</sup>/Cl<sup>-</sup>-dependent transporters. *Proc Natl Acad Sci U S A* **104**:12761-12766.
- Henry LK, Field JR, Adkins EM, Parnas ML, Vaughan RA, Zou MF, Newman AH, and Blakely RD (2006) Tyr-95 and Ile-172 in transmembrane segments 1 and 3 of

human serotonin transporters interact to establish high affinity recognition of antidepressants. *J Biol Chem* **281**:2012-2023.

Henry LK, Adkins EM, Han Q, and Blakely RD (2003) Serotonin and cocaine-sensitive inactivation of human serotonin transporters by methanethiosulfonates targeted to transmembrane domain I. *J Biol Chem* **278**:37052-37063.

Hertting G, and Axelrod J (1961) Fate of tritiated noradrenaline at the sympathetic nerve-endings. *Nature* **192**:172-173.

Jacobs MT, Zhang YW, Campbell SD, and Rudnick G (2007) Ibogaine, a noncompetitive inhibitor of serotonin transport, acts by stabilizing the cytoplasm-facing state of the transporter. *J Biol Chem* **282**:29441-29447.

Jardetzky O (1966) Simple allosteric model for membrane pumps. *Nature* **211**:969-970.

Just H, Sitte HH, Schmid JA, Freissmuth M, and Kudlacek O (2004) Identification of an additional interaction domain in transmembrane domains 11 and 12 that supports oligomer formation in the human serotonin transporter. *J Biol Chem* **279**:6650-6657.

Korkhov VM, Holy M, Freissmuth M, and Sitte HH (2006) The conserved glutamate (Glu136) in transmembrane domain 2 of the serotonin transporter is required for the conformational switch in the transport cycle. *J Biol Chem* **281**:13439-13448.

Korkhov VM, Milan-Lobo L, Zuber B, Farhan H, Schmid JA, Freissmuth M, and Sitte HH (2008) Peptide-based interactions with calnexin target misassembled membrane proteins into endoplasmic reticulum-derived multilamellar bodies. *J Mol Biol* **378**:337-352.

Laskowski RA, MacArthur MW, Moss DS, and Thornton JM (1993) PROCHECK: a program to check the stereochemical quality of protein structures. *J Appl Cryst* **26**:283-291.

Ressl S, Terwisscha van Scheltinga AC, Vorrhein C, Ott V, and Ziegler C (2009) Molecular basis of transport and regulation in the Na<sup>+</sup>/betaine symporter BetP. *Nature* **458**:47-52.

Schloss P, and Betz H (1995) Heterogeneity of antidepressant binding sites on the recombinant rat serotonin transporter SERT1. *Biochemistry* **34**:12590-12595.

Scholze P, Norregaard L, Singer EA, Freissmuth M, Gether U, and Sitte HH (2002) The role of zinc ions in reverse transport mediated by monoamine transporters. *J Biol Chem* **277**:21505-21513.

Schmid JA, Scholze P, Kudlacek O, Freissmuth M, Singer EA, and Sitte HH (2001) Oligomerization of the human serotonin transporter and of the rat GABA transporter 1 visualized by fluorescence resonance energy transfer microscopy in living cells. *J Biol Chem* **276**:3805-3810.

Schmitt KC, Mamidyala S, Biswas S, Dutta AK, and Reith ME (2010) Bivalent phenethylamines as novel dopamine transporter inhibitors: evidence for multiple substrate-binding sites in a single transporter. *J Neurochem* **112**:1605-1618.

Segel IH (1975) *Enzyme kinetics: behavior and analysis of rapid equilibrium and steady-state enzyme systems*. John Wiley & Sons, New York.

Seidel S, Singer EA, Just H, Farhan H, Scholze P, Kudlacek O, Holy M, Koppatz K, Krivanek P, Freissmuth M, and Sitte HH (2005) Amphetamines take two to tango: an

MOL #67538

oligomer-based counter-transport model of neurotransmitter transport explores the amphetamine action. *Mol Pharmacol* **67**:140-151.

Shi L, Quick M, Zhao Y, Weinstein H, and Javitch JA (2008) The mechanism of a neurotransmitter:sodium symporter--inward release of Na<sup>+</sup> and substrate is triggered by substrate in a second binding site. *Mol Cell* **30**:667-677.

Singh SK, Piscitelli CL, Yamashita A, and Gouaux E (2008) A competitive inhibitor traps LeuT in an open-to-out conformation. *Science* **322**:1655-1661.

Singh SK, Yamashita A, and Gouaux E (2007) Antidepressant binding site in a bacterial homologue of neurotransmitter transporters. *Nature* **448**:952-956.

Sitte HH, and Freissmuth M (2010) The reverse operation of Na(+)/Cl(-)-coupled neurotransmitter transporters--why amphetamines take two to tango. *J Neurochem* **112**:340-355.

Sucic S, Dallinger S, Zdrzil B, Weissensteiner R, Jørgensen TN, Holy M, Kudlacek O, Seidel S, Cha JH, Gether U, Newman AH, Ecker GF, Freissmuth M, and Sitte HH (2010) The N terminus of monoamine transporters is a lever required for the action of amphetamines. *J Biol Chem* **285**:10924-10938.

Tavoulari S, Forrest LR, and Rudnick G (2009) Fluoxetine (Prozac) binding to serotonin transporter is modulated by chloride and conformational changes. *J Neurosci* **29**:9635-9643.

White KJ, Kiser PD, Nichols DE, and Barker EL (2006) Engineered zinc-binding sites confirm proximity and orientation of transmembrane helices I and III in the human serotonin transporter. *Protein Sci.* **15**:2411-22.

Yamashita A, Singh SK, Kawate T, Jin Y, and Gouaux E (2005) Crystal structure of a bacterial homologue of Na<sup>+</sup>/Cl<sup>-</sup>-dependent neurotransmitter transporters. *Nature* **437**:215-223.

Zhou Z, Zhen J, Karpowich NK, Goetz RM, Law CJ, Reith ME, and Wang DN (2007) LeuT-desipramine structure reveals how antidepressants block neurotransmitter reuptake. *Science* **317**:1390-1393.

Zhou Z, Zhen J, Karpowich NK, Law CJ, Reith ME, and Wang DN (2009) Antidepressant specificity of serotonin transporter suggested by three LeuT-SSRI structures. *Nat Struct Mol Biol* **16**:652-657.

Zomot E, Bendahan A, Quick M, Zhao Y, Javitch JA, and Kanner BI (2007) Mechanism of chloride interaction with neurotransmitter:sodium symporters. *Nature* **449**:726-730.

MOL #67538

## FOOTNOTES

This work was supported by project program grants from the Austrian Science Fund FWF (SFB35, CCHD) and the Medical University of Vienna (CCHD). We thank Sacrament of Transition, Maribor, Slovenia, for the kind gift of ibogaine.

## FIGURE LEGENDS

### **Figure 1. Final clusters of docking poses of imipramine in the binding cavity of hSERT**

TMs 1 (red), 3 (dark red), 6 (orange), 8 (brown, semi-transparent) & 10 (cyan) are depicted in the absence of the remaining TMs for clarity. (a) Cluster 1 poses contains two distinct placements: (a) the nitrogen atom is placed near E<sup>493</sup>, (b) interaction of the nitrogen with D<sup>98</sup> is observed, both are analogous to the crystal structure 2Q72. (b) Cluster 2 poses; D<sup>98</sup> coordinates the charged nitrogen of imipramine and the hydrophobic ring system is placed into the hydrophobic region of the binding site. (c) Cluster 3 poses; the tricyclic ring system is placed in the outer vestibule and the amino propyl side chain reaches into binding site 1. Interactions have been identified using the ligand interactions feature (distance based) as implemented in MOE.

### **Figure 2. Cellular expression and functional characterization of wild type and mutant SERTs**

The cellular expression of wild type or mutant SERTs was examined by confocal laser scanning microscopy (a). Representative images of HEK293 cells (1\*10<sup>5</sup> cells/16 mm glass coverslip) stably expressing YFP-tagged transporters indicate that the expression pattern of mutated proteins is similar to that shown by the wild type SERT. (b) For saturation uptake experiments, HEK293 cells stably expressing wild type or mutant SERTs were seeded onto 48-well plates (0.5\*10<sup>5</sup> cells/well), 24 h prior to experiments. Cells were incubated with [<sup>3</sup>H]5-HT, with or without 10 μM paroxetine to determine non-specific uptake. The assay was conducted in duplicates and reaction stopped after 1 min

## MOL #67538

with ice-cold Krebs-HEPES buffer. Data, plotted according to the hyperbolic model, are shown as means of a representative experiment carried out in duplicates. **(c)** Imipramine binding to SERT<sup>WT</sup> and SERT<sup>Y95F</sup>: the incubation was performed in a final volume of 250  $\mu$ L for 15 min at 27 °C. Non-specific binding was determined in the presence of 3  $\mu$ M paroxetine and was  $\leq 10\%$  at the  $K_D$  concentration of SERT<sup>WT</sup>. Data are from a single experiment carried out in duplicate, which was repeated three times. Average  $B_{max}$ -values were  $3.6 \pm 0.1$  and  $4.0 \pm 0.3$  pmol/mg for SERT<sup>WT</sup> and SERT<sup>Y95F</sup>, respectively. The  $B_{max}$  of the mutant is likely to be underestimated: because of the low affinity of [<sup>3</sup>H]imipramine, some bound ligand dissociates during the separation artefact. This conjecture was verified by immunoblotting (insert) which shows substantially higher levels of SERT<sup>Y95F</sup> than of SERT<sup>WT</sup>. The immunoblot revealed two bands: the upper band corresponds to the mature, fully glycosylated form and the lower form to the core-glycosylated (ER-resident) form. **(d)** Inhibition of [<sup>3</sup>H]5-HT uptake by imipramine was determined in HEK293 stably expressing wild type and mutant SERTs. The cells were incubated with 0.1 nM [<sup>3</sup>H]5-HT and increasing concentrations of imipramine, in the presence or absence of 10  $\mu$ M paroxetine (to determine non-specific uptake). The data (n=3) were analysed as described under 'Methods' and plotted according to the sigmoidal model.

### **Figure 3. Most favored docking poses of TCAs onto hSERT**

Overlay of TCAs imipramine, desipramine, amitriptyline, clomipramine, carbamazepine and dihydrocarbamazepine as obtained by superposition of group 3 of docking poses. The ring system of the TCAs, carbamazepine, and dihydrocarbamazepine occupies the external vestibule and the basic side chain of the TCAs is pointing towards binding site 1.



MOL #67538

Furthermore, the dibenzazepine ring system is placed near a hydrophobic region (brown) of the protein.

**Figure 4. Carbamazepine is a low affinity SERT ligand that shares the binding site of imipramine and precludes amphetamine action on SERT**

Saturation of [<sup>3</sup>H]imipramine binding to SERT in the presence of increasing concentrations of carbamazepine: mean ± SEM (n=3) **(a)** Carbamazepine displaces [<sup>3</sup>H]imipramine at a K<sub>I</sub> predicted by the Cheng-Prusoff approximation for competitive inhibition **(b)** Schild plot from the data presented in panel **(a)** reveals the following parameters: slope = 1.13, r = 0.976 with an x-intercept = pK<sub>B</sub> = 2.03 for carbamazepine **(c)**. For release assays **(d)**, culture medium was removed from stably transfected HEK293 cells (40\*10<sup>4</sup> cells/well grown in 96-well plates on coverslips). The cells were preloaded with 0.4 μM [<sup>3</sup>H]serotonin or with 0.1 μM [<sup>3</sup>H]MPP<sup>+</sup> for 20 min at 37 °C in a final volume of 100 μl Krebs-HEPES buffer/well. The coverslips were placed into superfusing chambers and excess radioactivity washed out with Krebs-HEPES buffer at 25 °C, for 45 min at a perfusion rate of 0.7 ml/min. Upon achieving stable efflux, 2-min fractions were collected and data analysed as described in 'Methods'.

**Figure 5. Mutually non-exclusive binding of 5-HT to SERT in the presence of carbamazepine**

**(a)** Competition of [<sup>3</sup>H]imipramine binding to SERT at equilibrium was performed in duplicate incubations in an assay volume of 0.2 to 0.5 ml (adjusted appropriately to avoid

MOL #67538

radioligand depletion). Membrane preparations (8-25  $\mu\text{g}/\text{assay}$ ) from HEK293 cells stably expressing wild type SERT were incubated with the radioligand ( $\sim 2$  nM [ $^3\text{H}$ ]imipramine), the indicated concentrations of carbamazepine and increasing concentrations of 5-HT in buffer (20 mM Tris-HCl, 1 mM EDTA, 2 mM  $\text{MgCl}_2$ , 3 mM KCl, 120 mM NaCl, pH adjusted to 7.4). Non-specific binding was determined in the presence of 3  $\mu\text{M}$  paroxetine. **(b)** Data in **(a)** is transformed into a Dixon plot for 5-HT by expressing the reciprocal of [ $^3\text{H}$ ]imipramine bound ( $\text{pmol}\cdot\text{mg}^{-1}$ ) as a function of 5-HT at a fixed concentration of carbamazepine. Data are shown as means  $\pm$  SD of three independent experiments in duplicate

**Figure 6. Paroxetine binds to SERT in a mutually non-exclusive manner in the presence of carbamazepine but, amphetamines elicit mutual exclusivity with carbamazepine**

Competition of [ $^3\text{H}$ ]imipramine binding to SERT at equilibrium was performed in duplicate incubations in an assay volume of 0.2 to 0.5 ml (adjusted appropriately to avoid radioligand depletion). Membrane preparations (8-25  $\mu\text{g}/\text{assay}$ ) from HEK293 cells stably expressing wild type SERT were incubated with the radioligand ( $\sim 2$  nM [ $^3\text{H}$ ]imipramine), the indicated concentrations of carbamazepine and increasing concentrations of paroxetine, MDMA and PCA in buffer (20 mM Tris-HCl, 1 mM EDTA, 2 mM  $\text{MgCl}_2$ , 3 mM KCl, 120 mM NaCl, pH adjusted to 7.4). Non-specific binding was determined in the presence of 3  $\mu\text{M}$  paroxetine. The binding data from the competition experiments is transformed into a Dixon plot for paroxetine **(a)**, MDMA **(b)** and PCA **(c)** by expressing the reciprocal of [ $^3\text{H}$ ]imipramine bound ( $\text{pmol}\cdot\text{mg}^{-1}$ ) as a

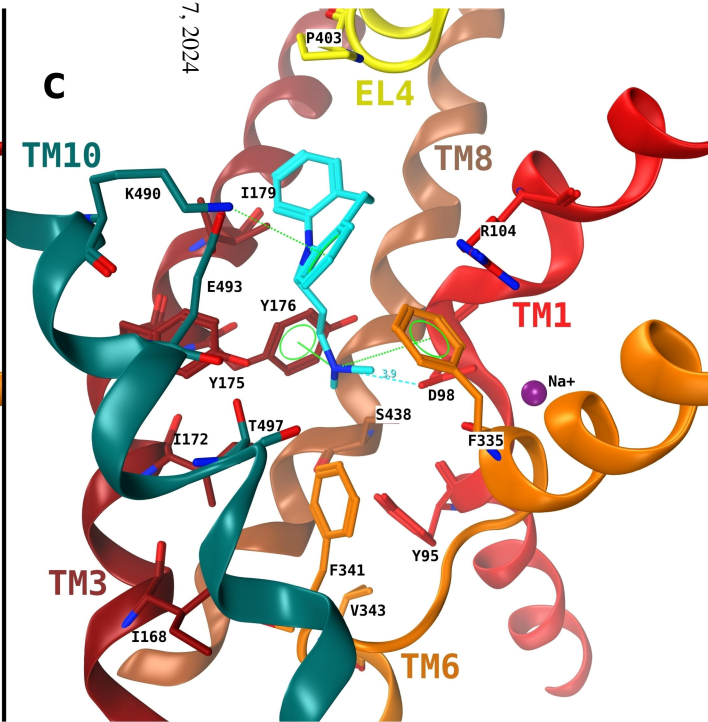
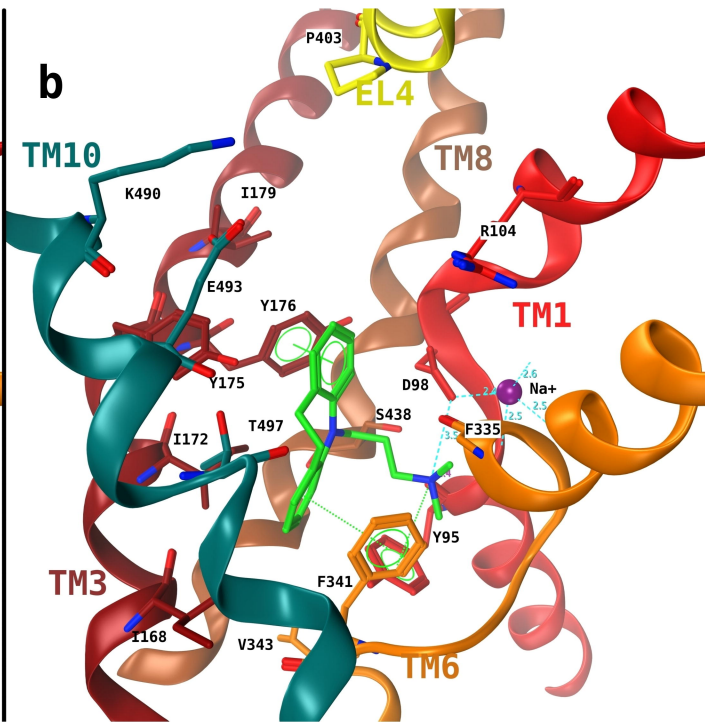
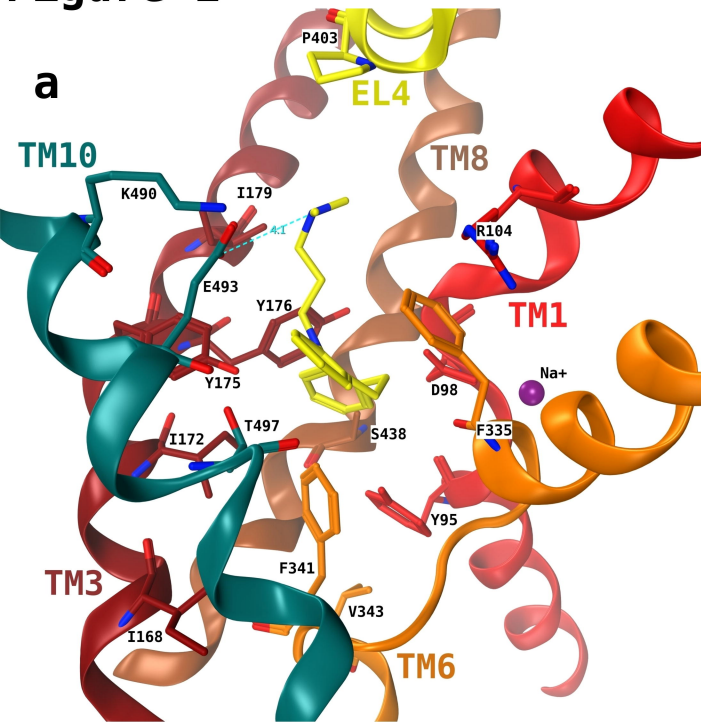
MOL #67538

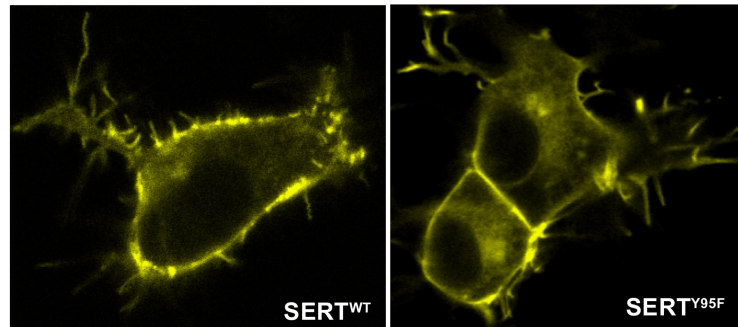
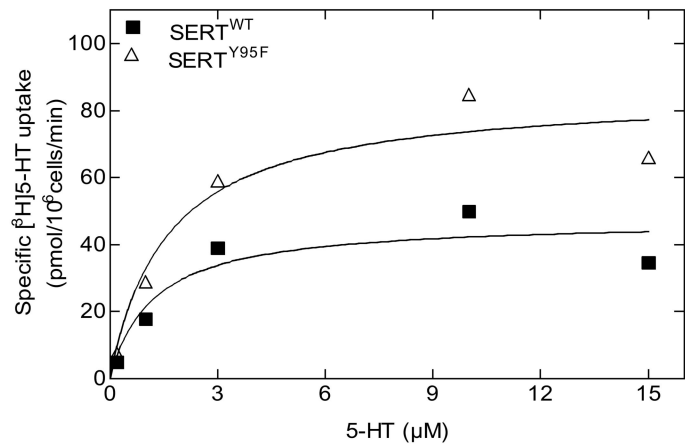
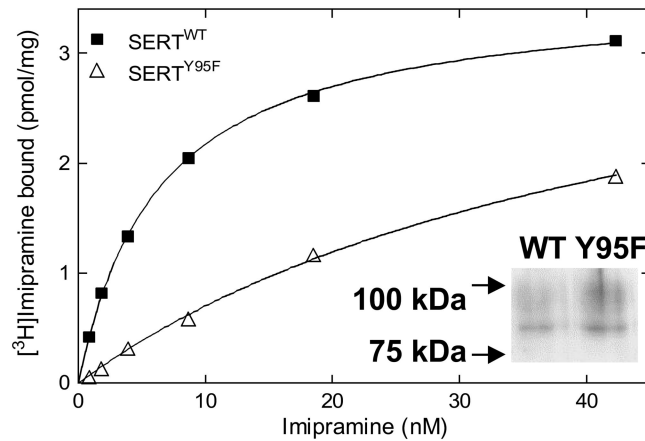
function of paroxetine, MDMA and PCA at a fixed concentration of carbamazepine, respectively. Data are shown as means  $\pm$  SD of three independent experiments in duplicate.

**Figure 7. Mutually non-exclusive binding of ibogaine to SERT and DAT in the presence of carbamazepine.**

Competition of [ $^3$ H]imipramine (**a**) or [ $^3$ H]WIN 35,428 (**c**) binding to SERT or DAT at equilibrium, respectively was performed in duplicate incubations in an assay volume of 0.2 to 0.5 ml (SERT) or 0.1ml (DAT). Membrane preparations (8-25  $\mu$ g/assay) from HEK293 cells stably expressing wild type SERT or DAT were incubated with the radioligand ( $\sim$ 2 nM [ $^3$ H]imipramine or  $\sim$ 10nM WIN 35,428), the indicated concentrations of carbamazepine and increasing concentrations of ibogaine in buffer (20 mM Tris-HCl, 1 mM EDTA, 2 mM MgCl<sub>2</sub>, 3 mM KCl, 120 mM NaCl, pH adjusted to 7.4). Buffers used for the preparation of DAT-expressing membranes contained 10  $\mu$ M ZnCl<sub>2</sub>-and were devoid of EDTA. Non-specific binding was determined in the presence of 3  $\mu$ M paroxetine (SERT) or 3  $\mu$ M methylphenidate (DAT). The binding data from the competition experiments is transformed into a Dixon plot for ibogaine (SERT) (**b**) and DAT (**d**) by expressing the reciprocal of [ $^3$ H]imipramine or [ $^3$ H]WIN 35,428 bound ( $\text{pmol}\cdot\text{mg}^{-1}$ ) as a function of ibogaine at a fixed concentration of carbamazepine, respectively.

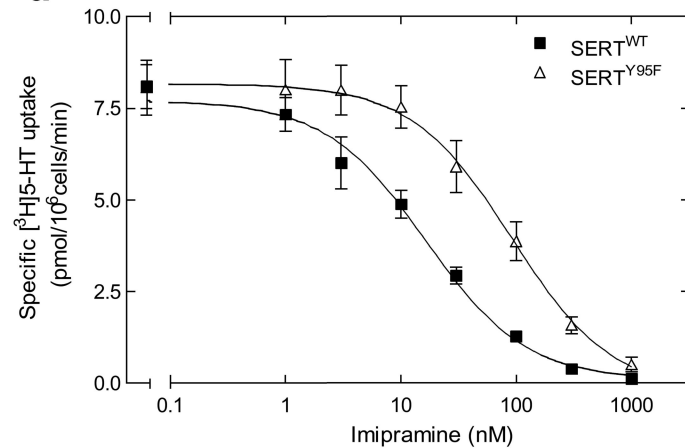
# Figure 1



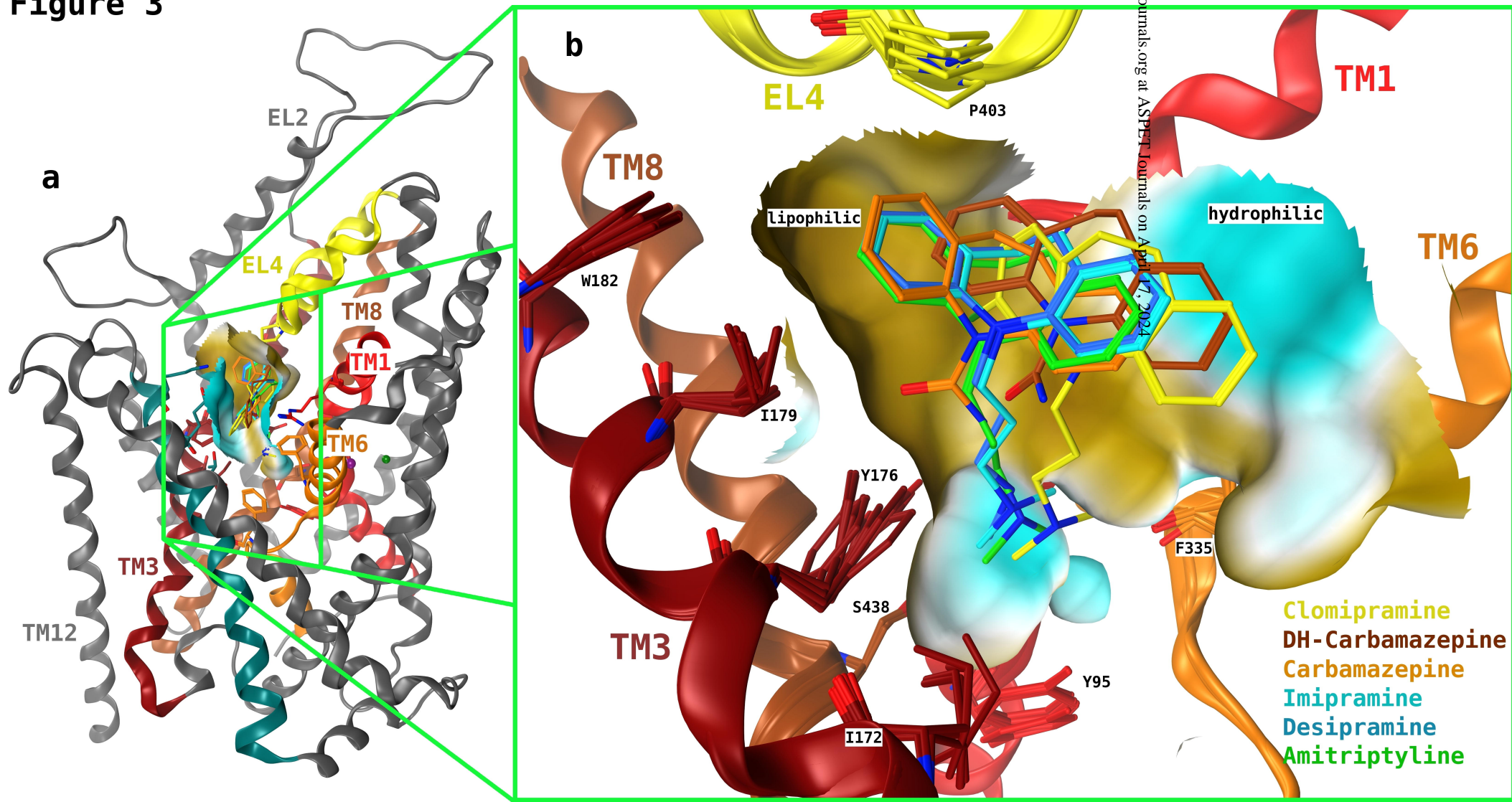
**Figure 2****a****b****c****WT****Y95F**

100 kDa →

75 kDa →

**d**

**Figure 3**



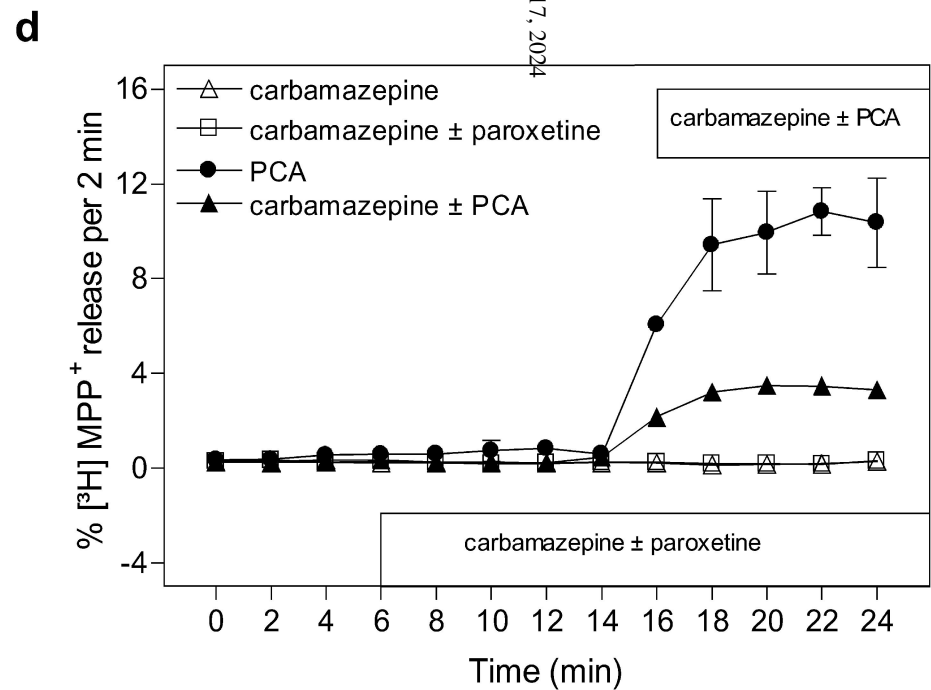
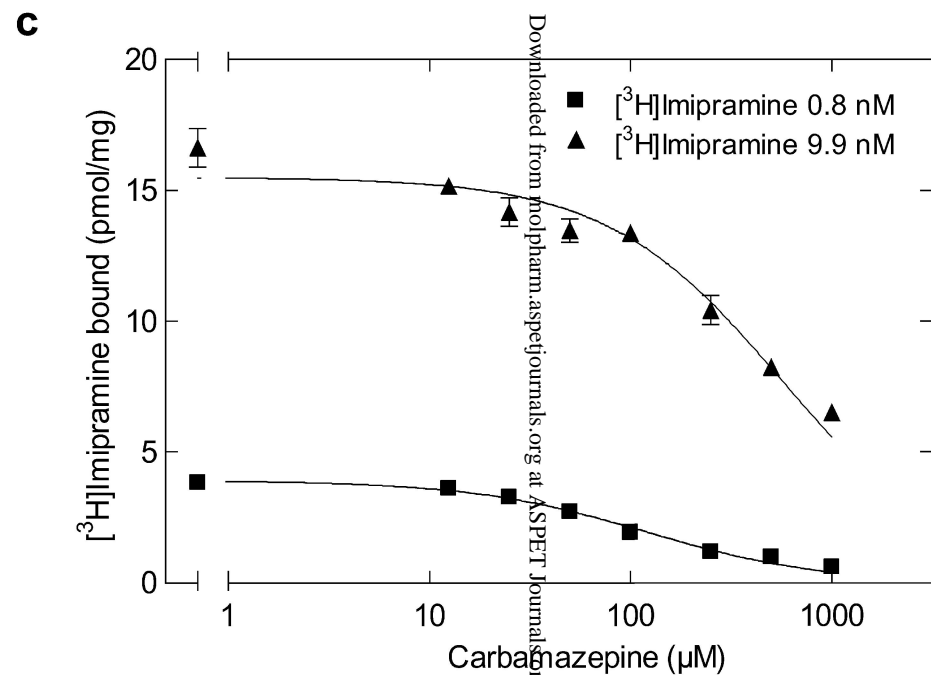
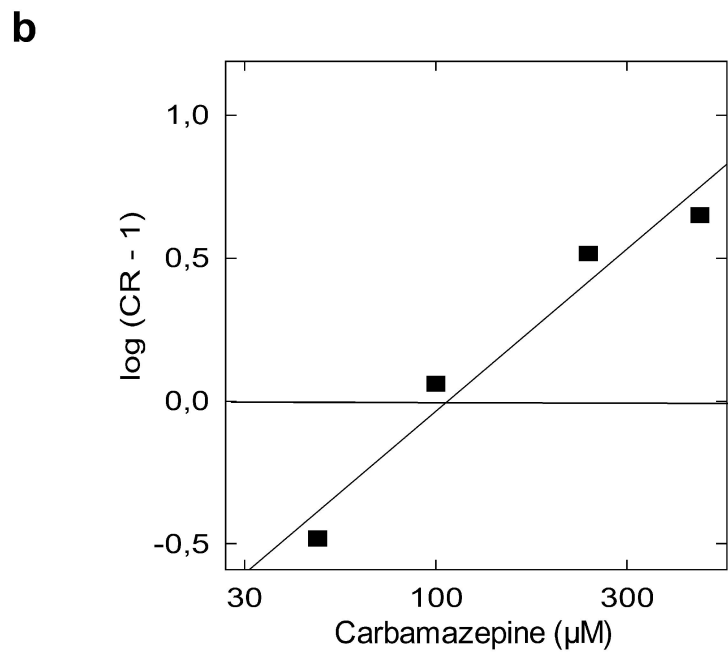
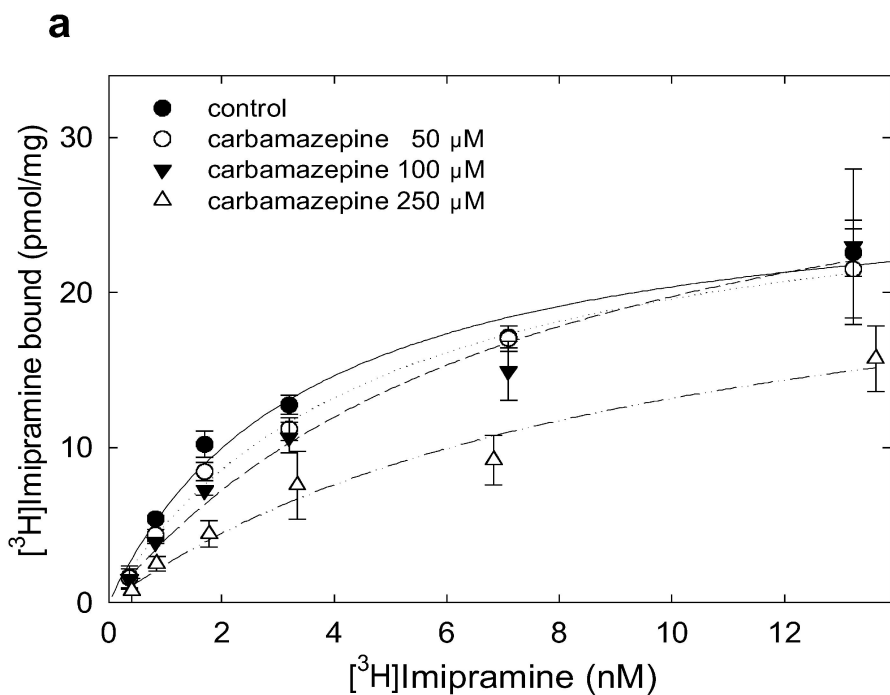
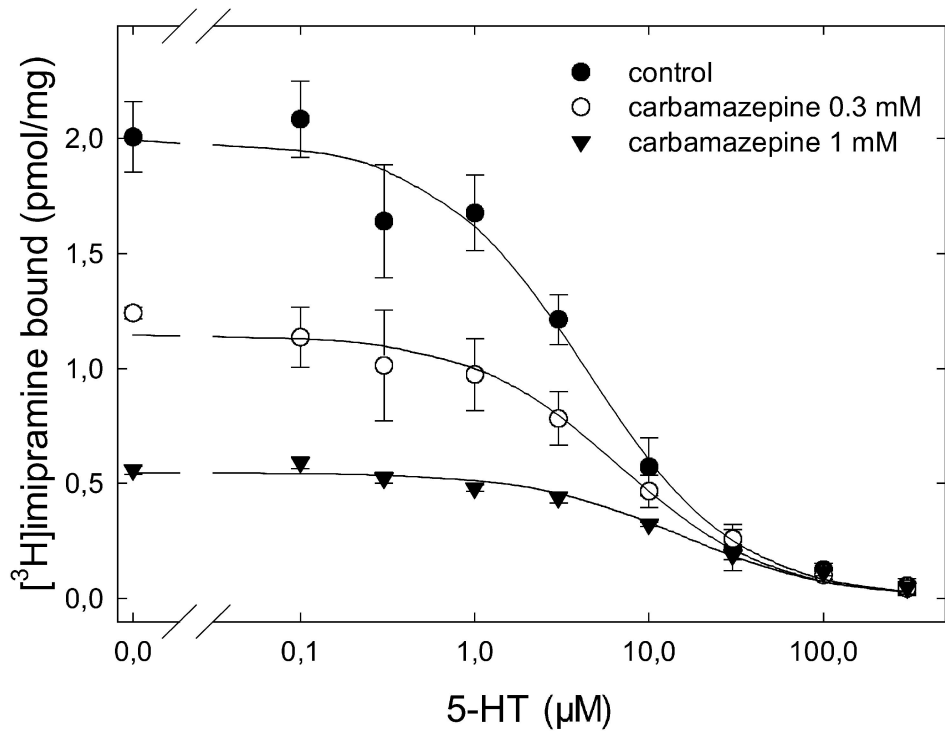
**Figure 4**

Figure 5

a



b

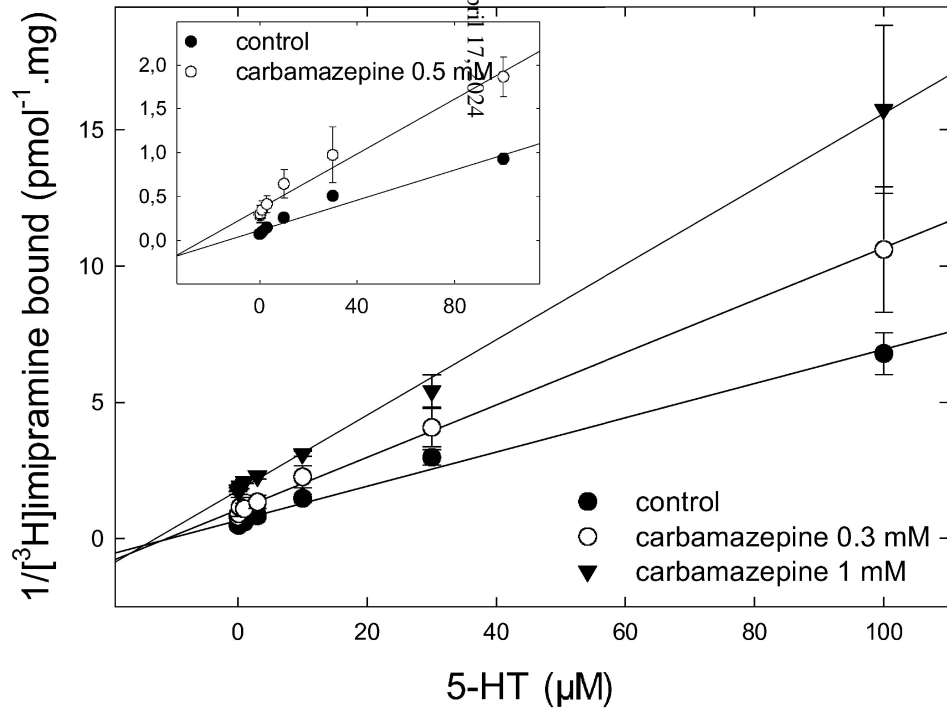
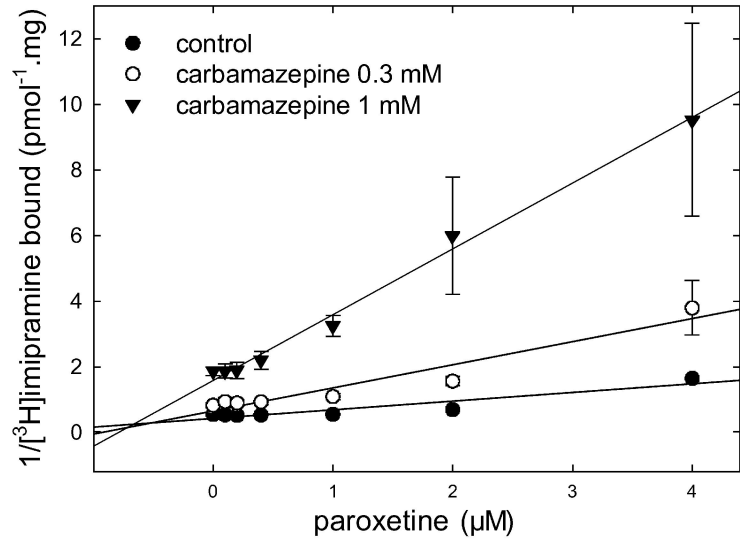


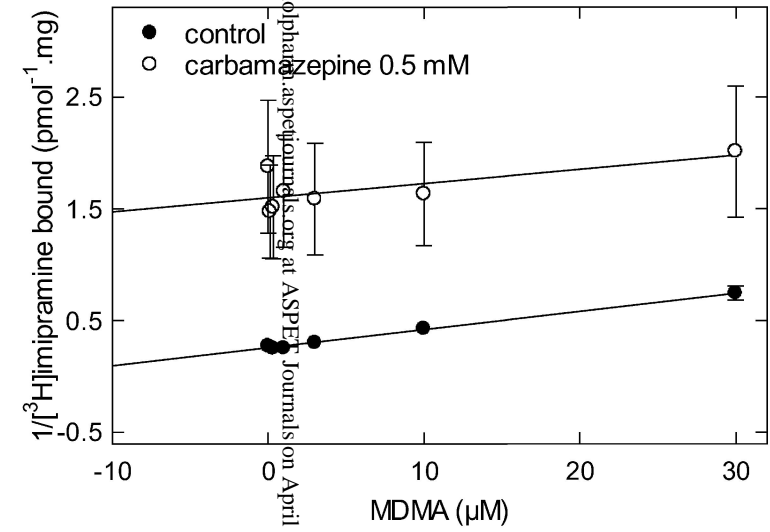


Figure 6

a



b



c

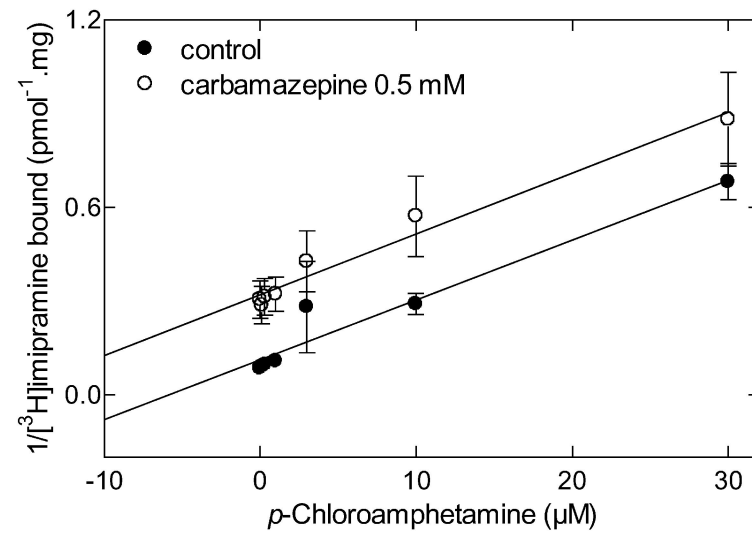
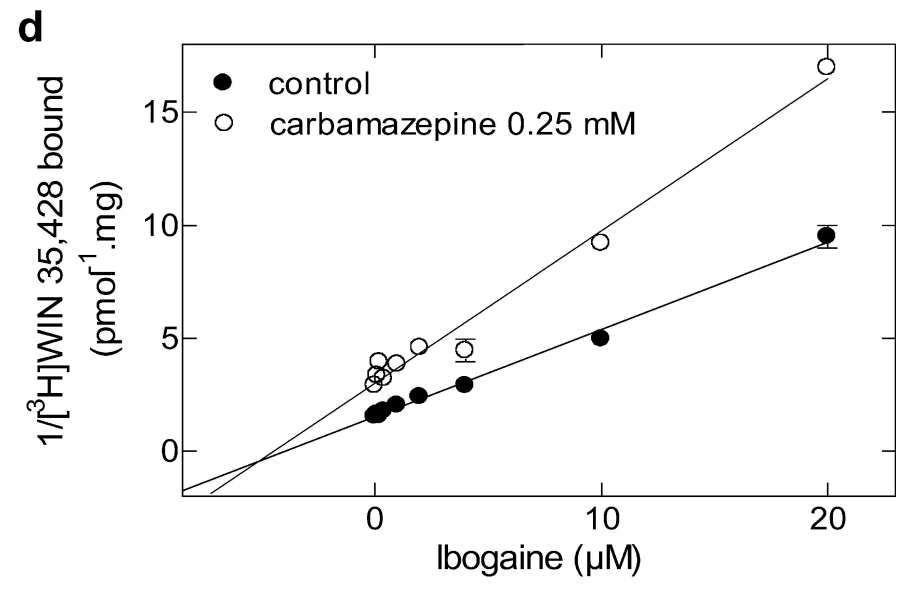
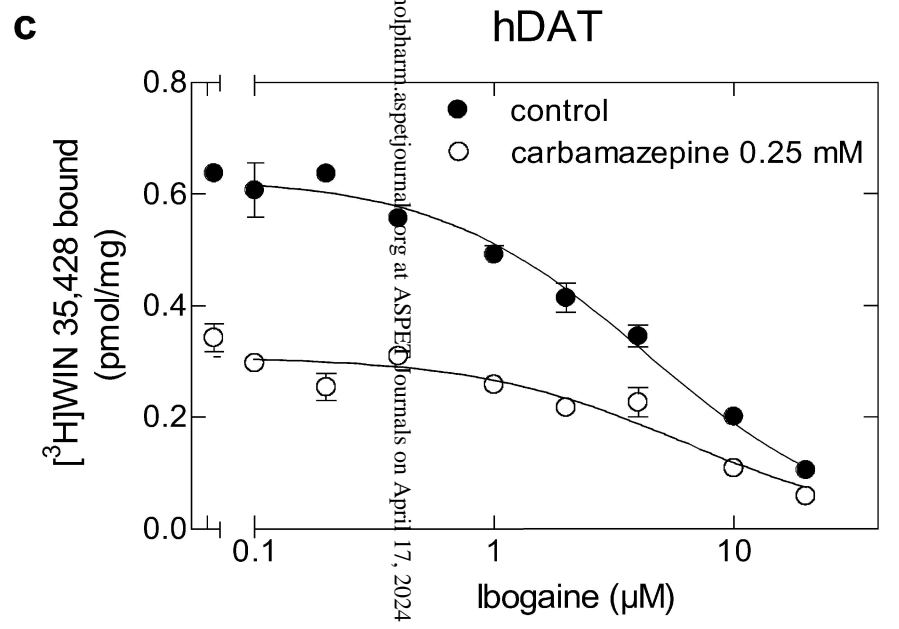
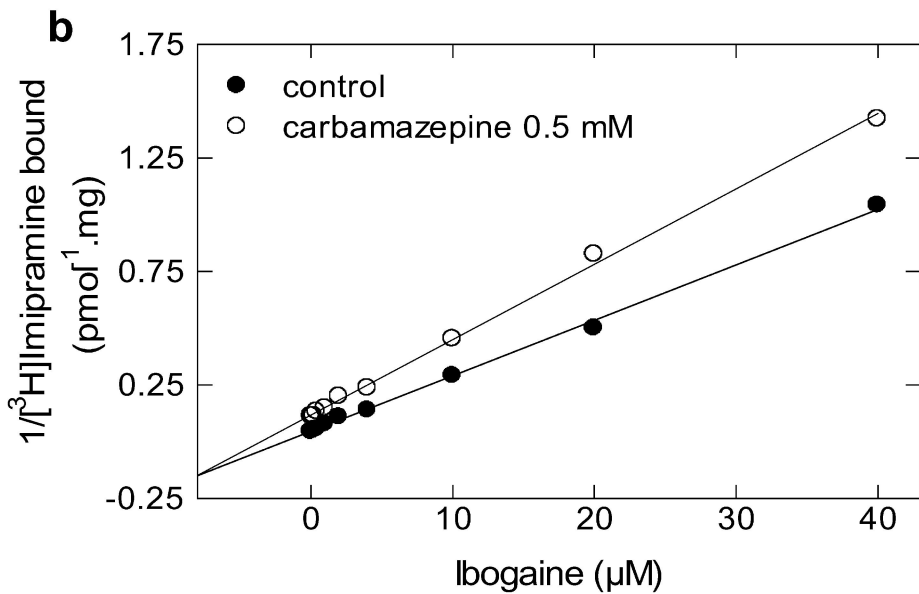
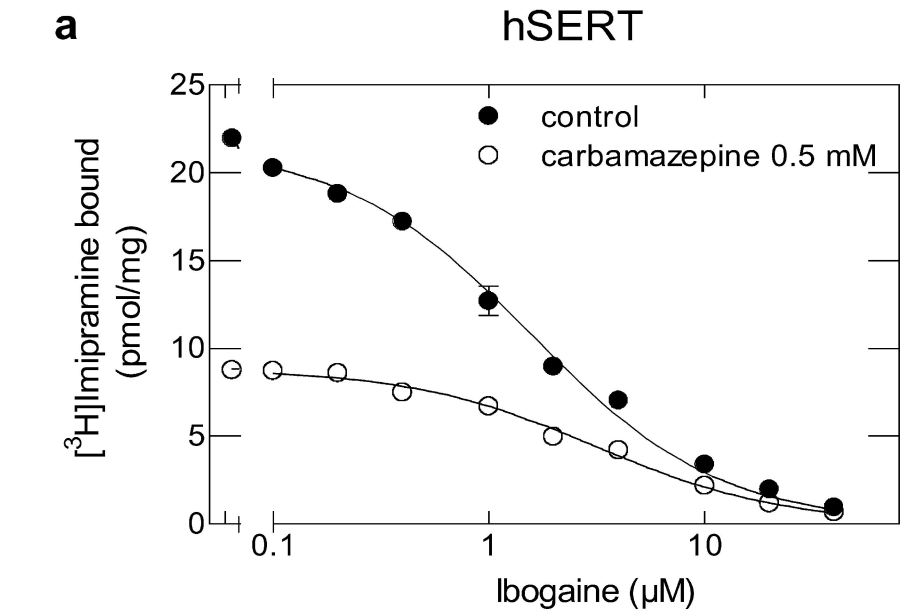


Figure 7



Downloaded from molpharm.aspetjournal.org at ASPEN Journals on April 17, 2024

THE HIGH-AFFINITY BINDING SITE FOR TRICYCLIC  
ANTIDEPRESSANTS RESIDES IN THE OUTER VESTIBULE OF THE  
SEROTONIN TRANSPORTER

Subhdeep Sarker, René Weissensteiner, Ilka Steiner, Harald H. Sitte,  
Gerhard F. Ecker, Michael Freissmuth\* and Sonja Sucic

Article submitted to the journal: Molecular Pharmacology

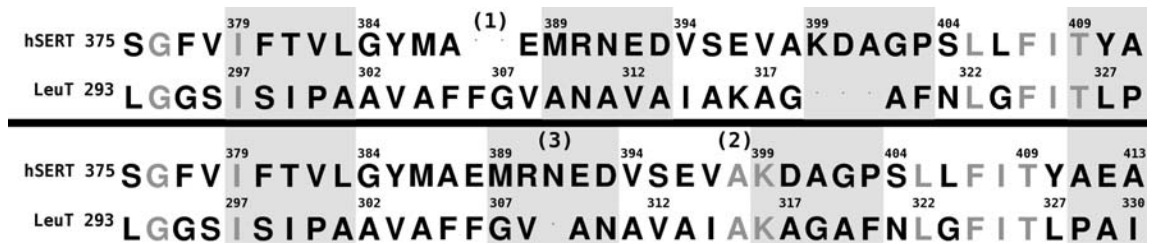
SS, IS, HHS, MF and SS are from the Institute of Pharmacology, Center for Physiology and  
Pharmacology, Medical University of Vienna, Waehringer Strasse 13a, A-1090 Vienna,  
Austria;

RW and GFE are from the Department of Medicinal Chemistry, University of Vienna,  
Althanstrasse 14, 1090 Vienna, Austria

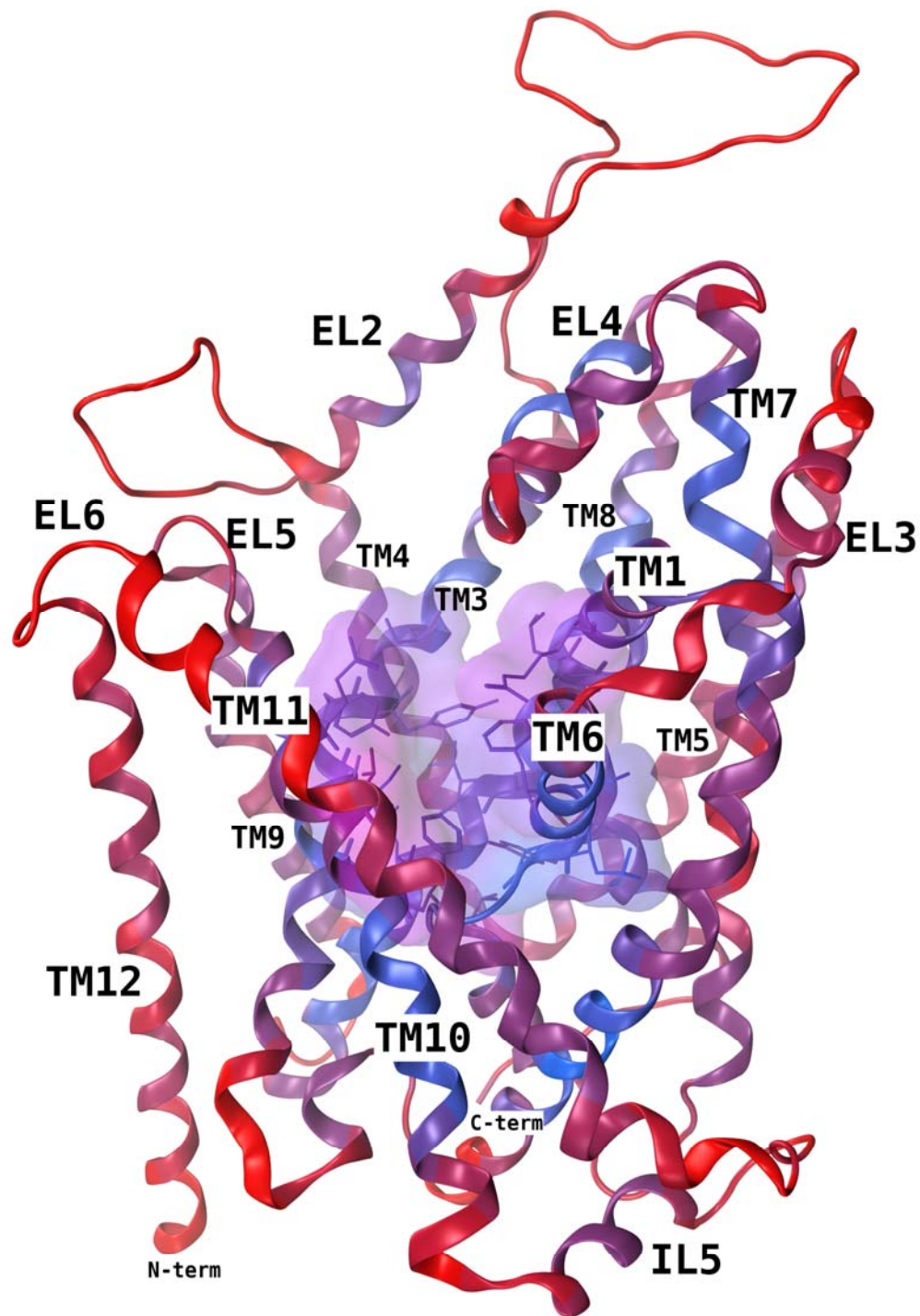
(a) Number of supplementary figures: 5

(b) Number of supplementary tables: 3

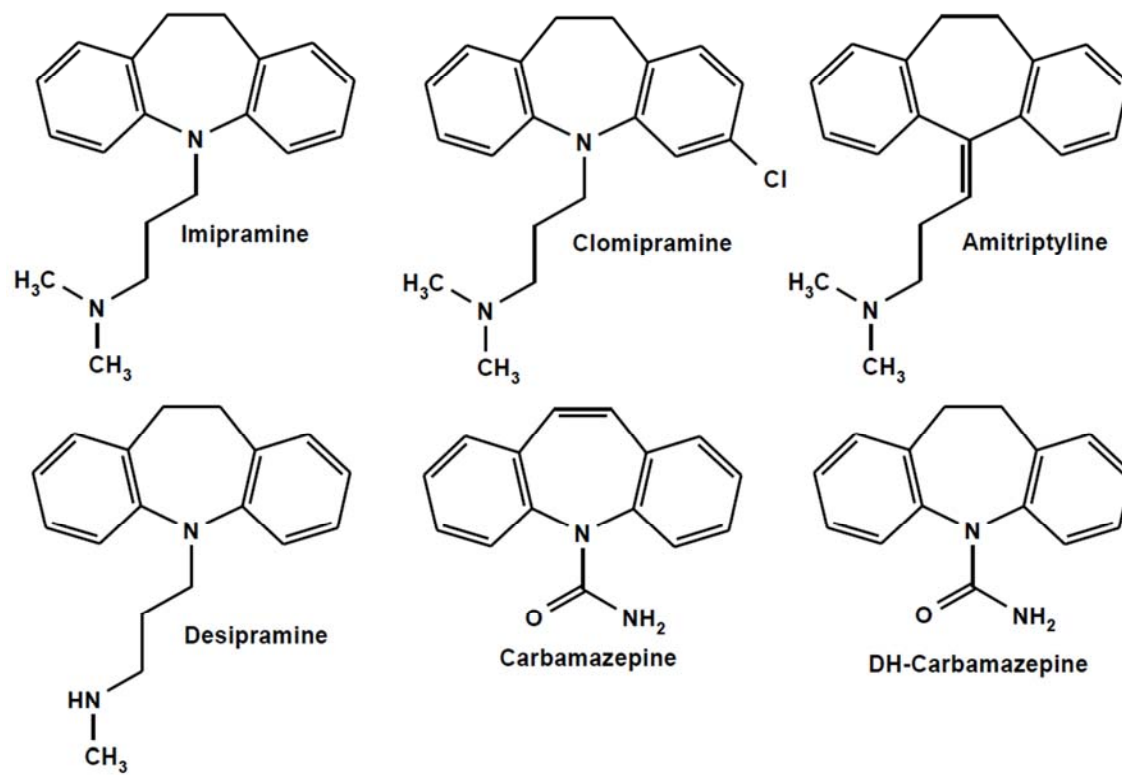
## Supplementary Material



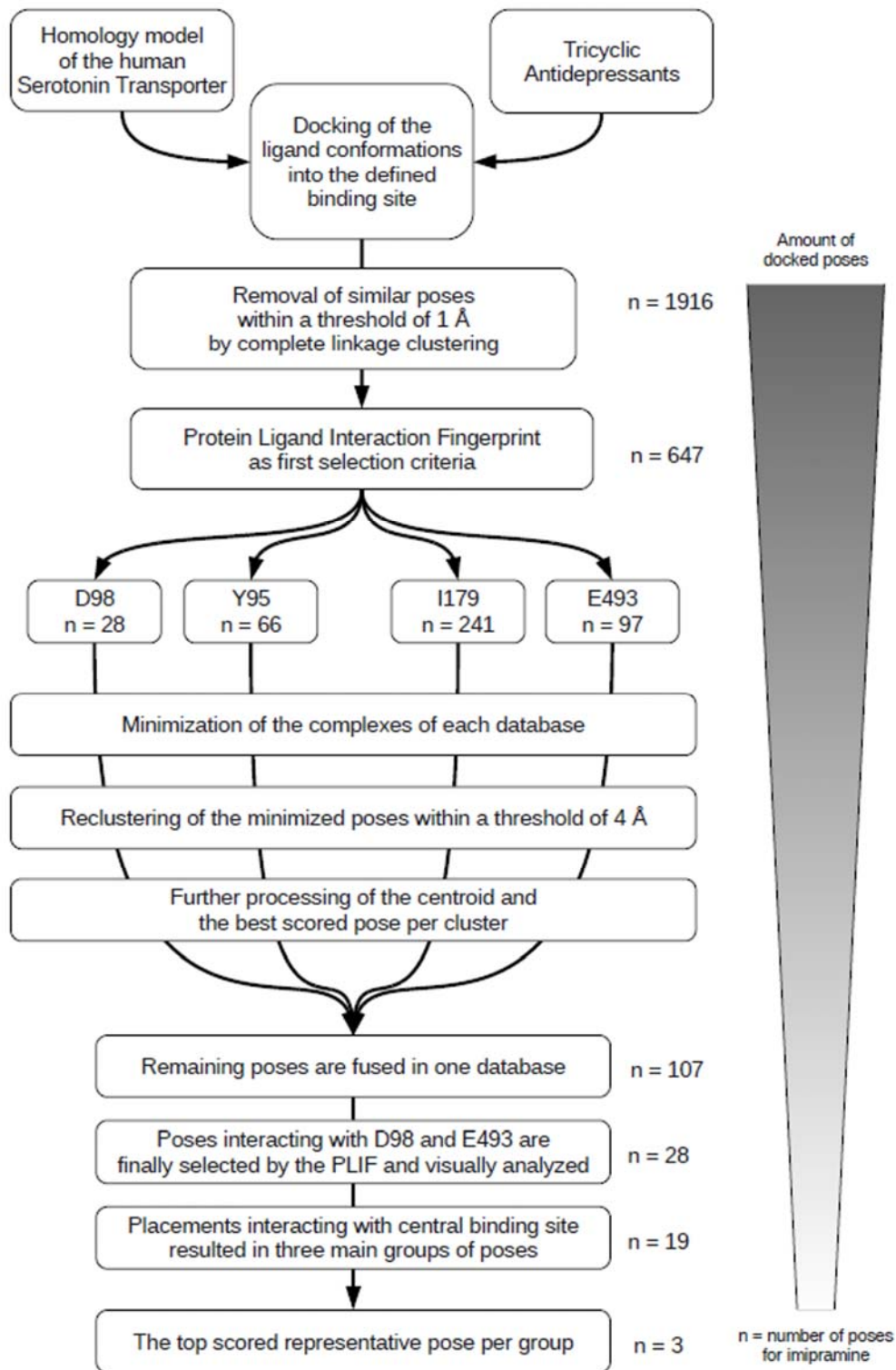
**Supplementary Figure 1:** Changes in the alignment compared to that published by Beuming et al. (Beuming et al. 2006). Upper row shows the original alignment. Bottom row outline the modified alignment. (1) In the query sequence a gap was removed, and (2) a match of A<sup>398</sup> and K<sup>399</sup> with the template was achieved. (3) N<sup>391</sup> was inserted into the template at the end of TM7.



**Supplementary Figure 2:** Homology model of hSERT coloured according to the result of the structural assessment by the QMEAN scoring function. Regions with high accuracy (estimated error <math>< 1 \text{ \AA}</math>) are depicted in blue. The red coloured regions show an estimated error of > 3.5 \text{ \AA}. Intermediate residues are depicted in magenta. The defined binding site is represented as transparent surface.



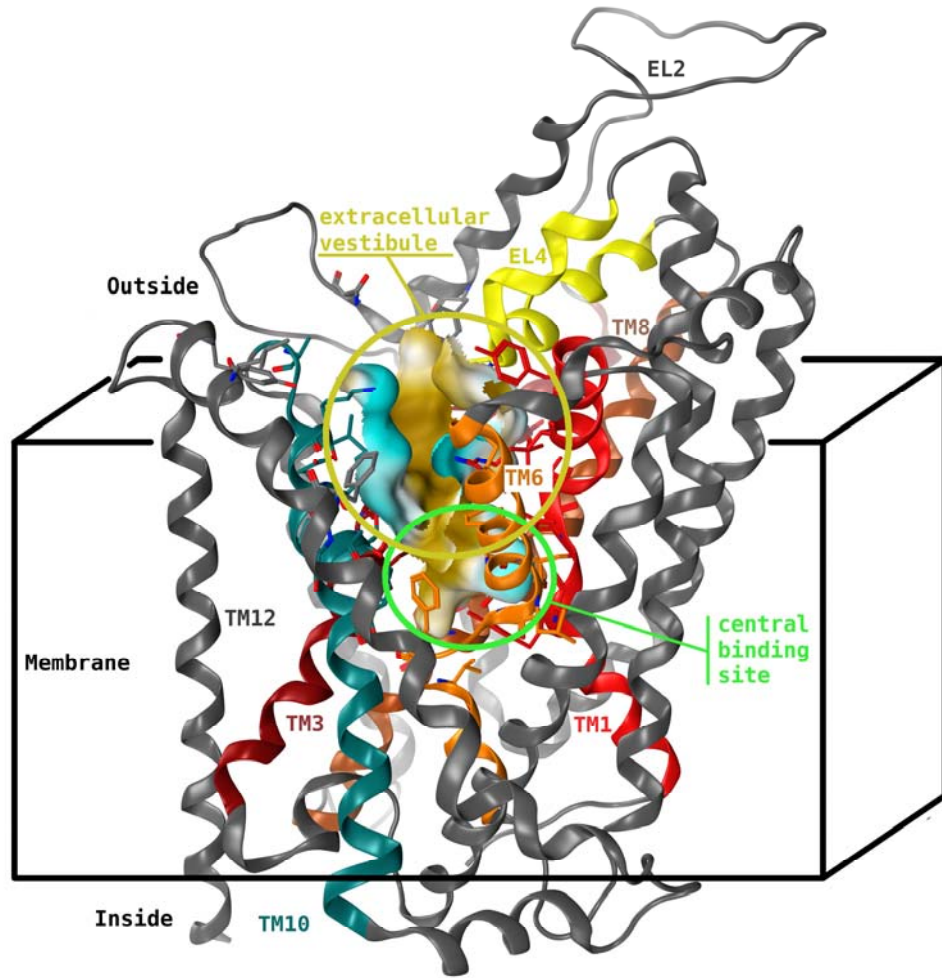
**Supplementary Figure 3:** Chemical structures of compounds used for the docking study.



**Supplementary Figure 4:** Protocol of the docking and evaluation procedure depicted as flow chart. The numbers on the right side correspond to the amount of poses of imipramine.







**Supplementary Figure 5:** The homology model of hSERT placed in a schematic membrane shows two distinct binding sites. In the 'open-to-out' conformations both sites are continuous and depicted as hydrophobicity surface (blue = hydrophilic, beige = lipophilic). Green circle: Central substrate binding site in the center of the transporter. Yellow circle: Extracellular vestibule and ligand entry path.

Supplementary Table 1: Mutagenesis studies used for validation of the homology model of hSERT

Publication	Residue	Criterion	fulfilled; comment
Andersen et al.	I179	in extracellular vestibule; part of the entrance	yes
	D400	in EL4; no effect or slight effect on inhibitor binding	yes; orientated towards extracellular medium
	S438	Important for recognition of substrate and inhibitors; near D98	yes
	L486	in extracellular vestibule; no effect or slight effect on inhibitor binding	yes
	V489	in extracellular vestibule; no effect or slight effect on inhibitor binding	yes
	K490	in extracellular vestibule; no effect or slight effect on inhibitor binding	no; group 3 shows pi-cation interaction
Barker et al.	D98	important for transporter function; is placed central in binding site 1	yes; coordinates one Na <sup>+</sup> and Ligands
Chen et al.	I172	MTS-accessible from both sites; protected by substrates and inhibitors	yes; located in central binding site
	I179	protected only by substrates; may be buried in hydrophobic environment	partly
Field et al.	T323	MTSEA-Biotin accessible	yes
	G324	MTSEA-Biotin accessible	yes
	I327	MTSEA-Biotin accessible	yes
	A331	MTSEA-Biotin accessible	yes
	I333	MTSEA-Biotin accessible, may distinguish between 5HT and MDMA	no; orientated towards TM2
	F334	MTSEA-Biotin accessible	yes
	F335	MTSEA-Biotin accessible	yes
	S336	MTSEA-Biotin accessible, coordination of Na, Cl, 5HT; opposed to N101	yes
	G338	domain movement - no function when mutated	located in unwound region
	G342	domain movement - no function when mutated	located in unwound region
F347	MTSEA-Biotin accessible	no; below central binding site	
Forrest et al.	Y95	accessible from both sides of the membrane	not in our 'open-to-out' model
	G442	not accessible; part of the central binding site	yes
	L443	not accessible; part of the central binding site	yes
Henry et al. 2003	D98	accessible, protected by 5HT	yes
	G100	accessible, protected by 5HT and Cocaine	yes
	N101	accessible, protected by 5HT and Cocaine	partly
	W103	not well accessible	yes
	Y107	accessible, protected by 5HT	partly, on the extracellular end of the helix
	I108	accessible	yes
Henry et al. 2006	Y95C/I172C	no Cd <sup>++</sup> binding site; too distant	yes
	N101C/I179C	Cd <sup>++</sup> binding site; close enough	no, too distant
	I172	located in the central binding site; involved in ligand binding	yes
	I179	indirectly involved in ligand binding	yes
White et al.	V102C/D98	Zn <sup>++</sup> binding site	partly; both residues are in proximity
	V102C/M180C	inhibited by MTS-3-MTS; suggesting a distance of 5 to 6.5 Å	orientation matches; distance larger
	V102C/A183C	disulphide bond	orientation matches; distance larger
	W103H/M180C	sensitive for Zn <sup>++</sup> inhibition; not W103C/M180C (too distant)	orientation matches; distance larger
	Distances (in Å) between the mentioned residues in the model of White et al.		distances measured from Cβ in our model
	V102-I179	8,5	13,3
	V102-M180	8,6	13,6
	V102-A181	n.d. - opposite side of the helix	opposite side of the helix
	V102-W182	9,9	14,1
	V102-V183	7,5	11,7
	V102-L184	n.d. - opposite side of the helix	opposite side of the helix

The homology model of hSERT was validated with mutagenesis studies. Concerning the location and orientation of residues important for ligand binding, most of the criteria are fulfilled.

Supplementary Table 2: Interactions of the docking poses of imipramine with residues of hSERT

Domain	Interacting Residue	Number of Hits	Type of Main Interaction	Number of Hits
TM1	Y95*	82	contact	Y95*
	A96*	4	backbone donor	A96*
	D98*	28	ionic	D98*
	L99*	0		L99*
	G100*	0		G100*
	R104*	218	contact	R104*
	Y107	31	contact	Y107
TM3	A169*	0		A169*
	I172*	0		I172*
	A173*	0		A173*
	Y175*	54	sidechain donor	Y175*
	Y176*	6	sidechain donor	Y176*
	I179*	243	contact	I179*
	W182	215	contact	W182
EL2	A183	27	contact	A183
	Y232	48	contact	Y232
TM6	Q238	5	contact	Q238
	D328	34	contact	D328
	F335*	50	contact	F335*
	S336*	3	backbone donor	S336*
	L337*	0		L337*
	G338*	0		G338*
	F341*	2	backbone donor	F341*
EL4	V343*	0		V343*
	P403	209	contact	P403
TM8	S438*	5	backbone donor	S438*
	T439*	0		T439*
	G442*	78	contact	G442*
	L443*	0		L443*
EL5	A486	5	contact	A486
TM10	V489	10	contact	V489
	K490	118	contact	K490
	E493*	454	contact	E493*
	E494	73	ionic	E494
	T497*	7	sidechain donor	T497*
	G498*	0		G498*
	P499	26	contact	P499
	V501*	0		V501*
	L502	12	contact	L502
TM11	F556	20	contact	F556
	Y563	6	contact	Y563
	Y568	4	contact	Y568
Na <sub>1</sub> *		0		

Amount and the type of the most frequent populated interactions of imipramine with residues of hSERT. The docking algorithm prefers placements in the extracellular vestibule near E493 and I179. Residues marked with an asterisk have been part of the defined binding site for docking.

Supplementary Table 3: Interactions of poses in group 3

Pose	Residue					
	D98	Y175	Y176	F335	K490	E493
1	ionic		$\pi$ -cation			
2*	ionic		$\pi$ -cation	$\pi$ -cation	$\pi$ -cation	
3	ionic					
4		H-bond				ionic
5	ionic				$\pi$ -cation	
6	ionic			$\pi$ -cation	$\pi$ -cation	
7	ionic		$\pi$ -cation			

The type of interactions of the docking poses in group 3 with residues of the homology model of hSERT were obtained by the function 'Ligand Interactions' implemented in MOE. (\*)Docking pose 2 as the top scored one of this group was finally selected as representative.